Chapter 13
Bifurcations

13.1 Introduction

We consider the following system of ordinary differential equations

$$\frac{dx}{dt} = \tilde{F}(x, \lambda), \tag{13.1}$$

where: $x \in \mathbb{R}^n$, $\lambda \in \mathbb{R}^k$, $\tilde{F} : \mathbb{R}^n \times \mathbb{R}^n \to \mathbb{R}^n$. The evolutionary system (13.1) can be represented by the vector field x_λ. A solution of the system (13.1) is defined by the phase flow $\Phi_\lambda : \mathbb{R}^k \times \mathbb{R}^n \to \mathbb{R}^n$, where $\Phi_\lambda(x, t) = x_\lambda(t)$ with the attached initial conditions $x = x_\lambda(0)$.

One can use a terminology introduced by Arnold [11]. An object depending on parameters is said to be a *family*. A small change of parameters leads to the object *deformations*. It appears that very often an analysis of all potential deformations is reduced to analysis of a representative one, further referred as a *versal deformation*. The latter can be found using a procedure of reducing a linear problem to that with a Jordan form matrix.

Each set of parameters λ is related to a special configuration of the phase space of the considered dynamical system. It can happen that for different values of $\lambda \in \mathbb{R}^k$, the system behaves qualitatively different. The hyperplanes separating different subspaces of the investigated phase space correspond to the bifurcation sets of parameters. It may happen also that these separating hyperplanes can possess a very complicated structure.

We have already considered a matrix with multiple eigenvalues and we have shown, how to reduce it to a Jordan canonical form. As it has been pointed by Arnold [11], in many engineering oriented sciences, when a matrix is approximately known the obtained results may be qualitatively different from expectations. It is caused by a fact that even a slight perturbation can easily destroy a Jordan canonical form.

J. Awrejcewicz, *Ordinary Differential Equations and Mechanical Systems*,
DOI 10.1007/978-3-319-07659-1_13

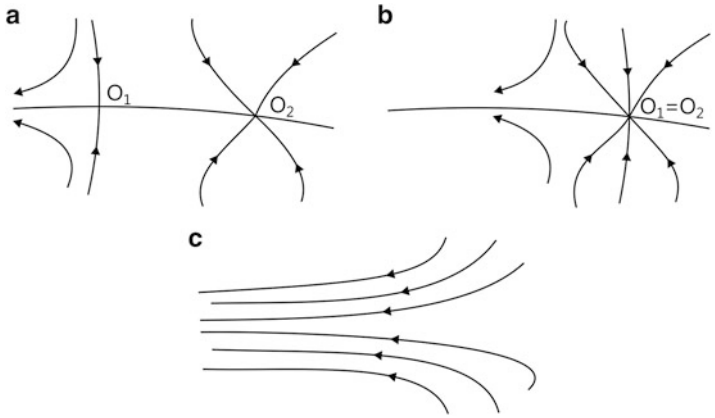

Fig. 13.1 Saddle-node bifurcation. The points O_1 and O_2 approach each other (**a**), overlap (**b**) and vanish (**c**)

However, in the case of parameterized families of matrices their perturbation does not change the multiple eigenvalue matrix form from the family. The problem defined by Arnold [11] is focused on a construction of the simplest form and to determine the minimum number of parameters to which a considered family can be reduced. A versal deformation is called *universal* if the change of the introduced transformation is determined uniquely. A versal deformation is *miniversal* one if the dimension of the parameter space is the smallest required to realize a versal deformation. The questions concerned a construction of miniversal deformations (normal forms) of matrices with multiple eigenvalues and the minimal number of parameters are also addressed in the monograph [243].

The main results are summed up in the following theorem.

Theorem 13.1. *Every matrix A possesses a miniversal deformation and the number of its parameters is equal to the codimension of the orbit of A.*

The smallest number of parameters of a versal deformation of the matrix A can be formally found following the steps given by Gantmacher [97] and Arnold [11].

To introduce a background of dynamical system bifurcations we briefly follow Neimark [181], who analysed some properties of two- and three-dimensional phase space bifurcations. In Fig. 13.1 three steps of the phase plain (portrait) changes are shown which refer to the saddle-node bifurcations. In Fig. 13.2 a situation when a stable focus changes lead to an occurrence of a periodic orbit is shown. In Fig. 13.3 three successive steps leading to occurrence of a stable and an unstable periodic orbits are shown. Note that doubled limit cycle creates the so-called critical orbit. In Fig. 13.4 the successive steps of an occurrence of a stable periodic orbit associated with a stable type separatrice is shown. In Fig. 13.5 three successive steps of a bifurcation changing the separatrices associated with two saddles are shown.

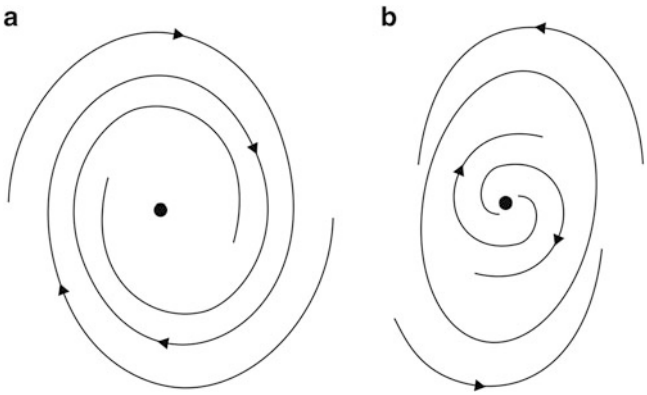

Fig. 13.2 Focus—periodic orbit bifurcation. A stable focus (**a**) becomes unstable and a stable periodic orbit is born (**b**)

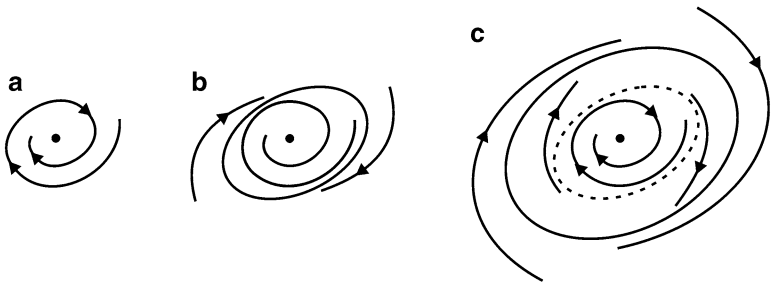

Fig. 13.3 Bifurcation leading to occurrence of two periodic orbits. A stable focus (**a**) becomes unstable and a stable periodic orbit is born (**b**), which eventually becomes also unstable and a second (stable) periodic orbit appears (**c**)

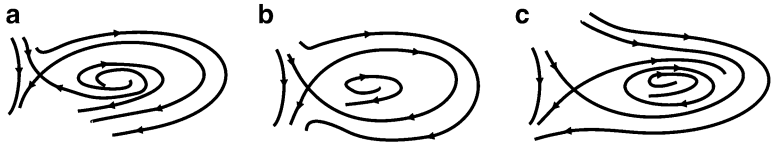

Fig. 13.4 Stable and unstable manifolds of a saddle (**a**) become closed (**b**) eventually leading to occurrence of a stable periodic orbit without a saddle point (**c**)

The dashed area corresponds to significant changes of the phase flow. Generally, bifurcations can be separated into two classes: static and dynamical bifurcations. *Static* bifurcations are related to equilibrium, whereas *dynamic* bifurcations are related to other objects of a phase space.

Recall that $\lambda \in \mathbb{R}^k$ and assume that the eigenvalues σ_i, related to a being investigated locally equilibrium (singular point) depend on $k-1$ *passive* parameters (scalars) and one *active* parameter λ^*. It is clear that for fixed passive parameters

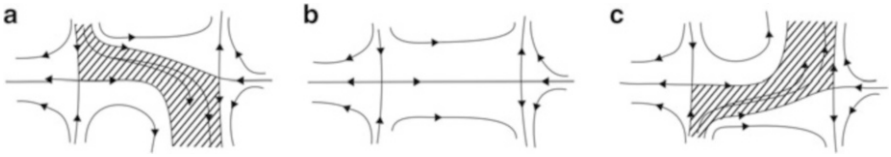

Fig. 13.5 Bifurcation changing separatrices of two saddles ((**a**) a trajectory before (**b**) in a critical state (**c**) and after bifurcation)

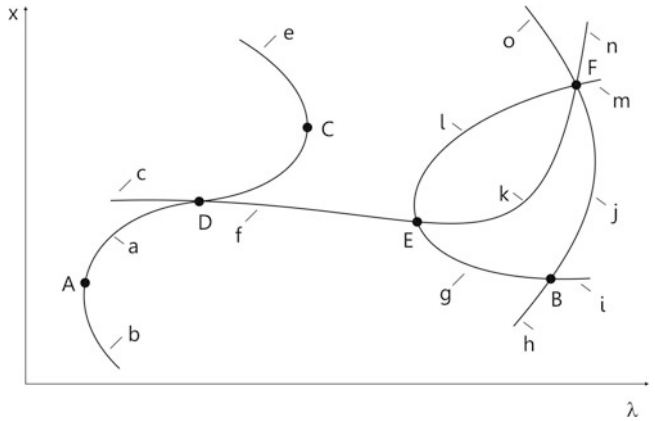

Fig. 13.6 Global bifurcation diagram

and for quasi-static changes of an active parameter one gets curves in the space $(\mathrm{Re}\,\sigma_i, \mathrm{Im}\,\sigma_i, \lambda^*)$, further called trajectories corresponding to the eigenvalues σ_i.

Suppose that increasing λ^* one of the eigenvalues crosses origin (an investigated equilibrium) and other eigenvalues remain either in left-hand side plane (LHP) or right-hand side plane (RHP). A small change of $\pm\Delta\lambda$ close to λ^* results in $\lambda^* \pm \Delta\lambda$. Two situations are possible. If a being investigated equilibrium changes its stability when λ^* changes from $\lambda^* - \Delta\lambda$ to $\lambda^* + \Delta\lambda$ and the leading eigenvalue remains always real then this bifurcation is called *divergence*.

The Hopf (or *flatter*) bifurcation occurs when a pair of complex conjugate eigenvalues crosses (with nonzero velocity) the imaginary axis of the plane $(\mathrm{Re}\,\sigma, \mathrm{Im}\,\sigma)$. The previously stable equilibrium becomes unstable and a new periodic orbit is born. A divergence belongs to one-dimensional bifurcation whereas Hopf bifurcation is two-dimensional one.

Note that although Hopf [124] stated the theorem valid for n-dimensional vector field, the sources related to this problem can be found in the work of Poincaré [202], and the first study of two-dimensional vector fields including a theorem formulation belongs to Andronov [8]. Hence some authors (see [243] for example) call this bifurcation as the Poincaré–Andronov–Hopf one.

In order to introduce a fundamental background of bifurcations we follow the diagram shown in Fig. 13.6 (see also Iooss and Joseph [127]).

The global bifurcation diagram includes branches of solutions (small letters) and branching points (capital letters). A *solution branch* corresponds to the uniqueness of the dependence $x(\lambda)$. However there may exist points where the uniqueness dependence is violated. They are called branching points. One also distinguishes *primary* branching points (A—limiting point, B—bifurcation point) and *secondary* bifurcation points (D—tangent point; C—limiting point; E—bifurcation point; F—multiple bifurcation point).

Consider two solutions $x(\lambda_0)$ and $x(\lambda_0) + \varepsilon$ of Eq. (13.1). Both of them satisfy the equations

$$\begin{aligned} \frac{dx(\lambda_0)}{dt} &= \tilde{F}(\lambda_0, x(\lambda_0)), \\ \frac{d(x(\lambda_0) + \varepsilon)}{dt} &= \tilde{F}(\lambda_0, x(\lambda_0) + \varepsilon). \end{aligned} \tag{13.2}$$

Hence in order to analyse equilibria states we obtain

$$F(\lambda, \varepsilon) = 0, \tag{13.3}$$

where $F(\lambda, \varepsilon) = \tilde{F}(\lambda_0, x(\lambda_0) + \varepsilon) - \tilde{F}(\lambda_0, x(\lambda_0))$.

The isolated solutions of Eq. (13.3) can be classified in the following way [127]:

1. *Regular* point. In this point derivative $F_\lambda \neq 0$ or $F_\varepsilon \neq 0$ and from the implicit function theorem one can find either a curve $\lambda(\varepsilon)$ or $\varepsilon(\lambda)$.
2. *Regular limiting* point. In this point $\lambda_\varepsilon(\varepsilon)$ changes its sign and $F_\lambda(\lambda, \varepsilon) \neq 0$.
3. *Singular* point. In this point $F_\lambda = F_\varepsilon = 0$
4. *Double bifurcation* point. In this point two curves with different tangents intersect each other.
5. *Bifurcation-limiting* point. In this double point the derivative λ_ε changes its sign.
6. *Tangent* point. This is a common point of two curves with the same tangent.
7. *Higher order singular* point. In this point first- and second-order derivatives are equal to zero.

13.2 Singular Points in 1D and 2D Vector Fields

13.2.1 1D Vector Fields

Our attention is focused on a first-order ordinary differential equation with one parameter λ of the form (13.1). For real values of both x and λ values the singular points (equilibria) are defined by the algebraic equation (13.3).

We are going to analyse an existence and uniqueness of singular points qualitatively including a construction of bifurcating solutions together with their stability estimation. Note that (in general) considering an implicit function (13.3) one can

get either the function $x(\lambda)$ or $\lambda(x)$, or isolated points, or it cannot be explicitly described. Here, following the earlier introduced classification given in Sect. 13.1, one deals either with *regular* or *singular* points. A regular point belongs to only one curve, whereas a singular point can be either isolated or it can belong to a few curves (branches). An order of singularity defines number of the associated branches. Here we would like briefly to explain a word "singular". It appears first as the name of equilibria of the dynamical systems. However, it appears second time when a nonlinear algebraic equation is considered and it concerns a classification of the roots of the algebraic equation.

The classification of equilibria results from the implicit function theorem.

Theorem 13.2. *Given the function $f(x, y)$ with continuous partial derivatives in the neighbourhood of (x_0, y_0), where $f(x_0, y_0) = 0$. If either $f_x(x_0, y_0) \neq 0$ or $f_y(x_0, y_0) \neq 0$, then:*

(i) There exists such α and β that for $x_0 - \alpha < x < x_0 + \alpha$, (or for $y_0 - \beta < y < y_0 + \beta$) we have a unique solution $y = y(x)$ (or $x = x(y)$);

(ii) The function $y = y(x)$ (or $x = x(y)$) is differentiable in the neighbourhood $|x - x_0| < \alpha$ (or $|y - y_0| < \beta$), and $\frac{dy}{dx}(x) = -\frac{f_x(x,y(x))}{f_y(x,y(x))}$ (or $\frac{dx}{dy}(y) = -\frac{f_y(x(y),y)}{f_x(x(y),y)}$).

Now we can define the singular points more precisely. A point (λ_0, x_0) is said to be *regular*, if both partial derivatives of the function $F(\lambda, x)$ are not simultaneously equal to zero, i.e.

$$F_\lambda^2(\lambda_0, x_0) + F_x^2(\lambda_0, x_0) \neq 0 \tag{13.4}$$

A regular point for which $F_x(\lambda_0, x_0) = 0$ is called the *extremal* point (it can be either minimum or maximum). A point for which (13.4) does not hold is said to be *singular*. A point (λ_0, x_0) is said to be singular of nth order, if the associated with this point derivatives up to the order $n - 1$ are equal to zero and at least one of the nth order derivatives is different from zero.

The solution branches are defined by the Taylor series. Introducing the new function $v = \frac{\lambda - \lambda_0}{x - x_0}$ and $w = \frac{x - x_0}{\lambda - \lambda_0}$ and dividing the Taylor series representation of $F(x, \lambda) = 0$ by $\frac{(x-x_0)^n}{n!}$ and by $\frac{(\lambda-\lambda_0)^n}{n!}$, we obtain the following nth order algebraic equations,

$$\begin{aligned} &A_0 v^n + A_1 v^{n-1} + \cdots + A_{n-1} v + A_n + O(\lambda - \lambda_0) = 0, \\ &A_0 + A_1 w + \cdots + A_{n-1} w^{n-1} + A_n w^n + O(x - x_0) = 0, \end{aligned} \tag{13.5}$$

where: $A_i = \frac{\partial^n F}{\partial x^i \partial \lambda^{n-i}}(\lambda_0, x_0)$, $i = 1, 2, \ldots, n$.

In a limit case $(\lambda, x) \to (\lambda_0, x_0)$ the algebraic equations with $O(\lambda - \lambda_0) = O(x - x_0) = 0$ serve to find a tangent of a slope to a solution branch to the axis x or λ, respectively. An existence of n solutions to Eq. (13.5) yields n different branches (some of them, however, can be degenerated). Real distinct solutions

correspond to distinct intersecting branches, whereas multiple solutions correspond to same tangent values of different solutions in the point (λ_0, x_0) or overlapping of multiple branches. Complex solutions correspond to the so-called degenerated branches (points) [144].

A point (λ_0, x_0) is called *degenerated* if it belongs simultaneously to degenerated branches (solutions).

An order of degeneracy of a singular point (λ_0, x_0) is defined by a number of complex roots of Eq. (13.5). In words, degeneracy order corresponds to a number of degenerated branches. Following the approach given in monograph [144] consider the first equation of the system (13.5), further referred as $H(\nu, \varepsilon) = 0$, where $\varepsilon = \lambda - \lambda_0$. Let ν_{0i} be solutions to the first equation of (13.5). A unique solution with the tangent ν_{0i} is obtained when $H_\nu(\nu_{0i}, 0) \neq 0$. This holds when ν_{0i} is a simple root of $H(\nu_{0i}, \varepsilon) = 0$. Note that in order to distinguish different tangent and identical branches passing through the point (λ_0, x_0) one needs to calculate higher order derivatives, which for instance define curvatures of the branches.

If $A_0, A_1, \ldots, A_{n-1}$ are equal to zero, then the first equation of (13.5) has $n - k$ roots, whereas the second possesses k roots equal to zero. Geometrically, it means that k branches have a tangent parallel to the axis λ in the point (λ_0, x_0). Now we briefly outline a construction of a solution branch in vicinity of the singular point (λ_0, x_0), for which

$$F(\lambda_0, x_0) = 0. \tag{13.6}$$

Let us approximate function F by its double Taylor series of the form (we follow here the approach given in monograph [144]):

$$\begin{aligned} F(\lambda, x) &= \alpha(\lambda) + a(\lambda)(x - x_0) + \frac{1}{2!}b(\lambda)(x - x_0)^2 + \frac{1}{3!}c(\lambda)(x - x_0)^3 + \cdots \\ &= \alpha_0 + \alpha_1(\lambda - \lambda_0) + \frac{1}{2!}\alpha_2(\lambda - \lambda_0)^2 + \frac{1}{3!}\alpha_3(\lambda - \lambda_0)^3 + \cdots \\ &\quad + [a_0 + a_1(\lambda - \lambda_0) + \frac{1}{2!}a_2(\lambda - \lambda_0)^2 + \frac{1}{3!}a_3(\lambda - \lambda_0)^3 + \cdots](\lambda - \lambda_0) \\ &\quad + \frac{1}{2!}[b_0 + b_1(\lambda - \lambda_0) + \frac{1}{2!}b_2(\lambda - \lambda_0)^2 \\ &\quad + \frac{1}{3!}b_3(\lambda - \lambda_0)^3 + \cdots](\lambda - \lambda_0)^2 + \frac{1}{3!}[c_0 + c_1(\lambda - \lambda_0) + \frac{1}{2!}c_2(\lambda - \lambda_0)^2 \\ &\quad + \frac{1}{3!}c_3(\lambda - \lambda_0)^3 + \cdots](\lambda - \lambda_0)^3 + \cdots, \end{aligned} \tag{13.7}$$

where: $\alpha_i = \frac{\partial^i F}{\partial \lambda^i}(\lambda_0, x_0)$, $a_i = \frac{\partial^{i+1} F}{\partial x \partial \lambda^i}(\lambda_0, x_0)$, $b_i = \frac{\partial^{i+2} F}{\partial x^2 \partial \lambda^i}(\lambda_0, x_0)$, $c_i = \frac{\partial^{i+3} F}{\partial x^3 \partial \lambda^i}(\lambda_0, x_0)$, and so on. Note that $\alpha_0 = 0$. If $F(\lambda, x_0) = 0$ (independently of λ) then $x = x_0$ is a solution. In addition, if (λ_0, x_0) is a regular point then $x = x_0$ is only one solution. However, if (λ_0, x_0) is a singular point then in spite of $x = x_0$ there may exist also additional branches of solutions. If $x - x_0 = \varepsilon$, then a solution can be parameterized by

$$\lambda - \lambda_0 = \varphi(\varepsilon), \tag{13.8}$$

where $\varphi(\varepsilon)$ can be approximated by the series

$$\varphi(\varepsilon) = \mu_0 + \mu_1\varepsilon + \mu_2\varepsilon^2 + \cdots \tag{13.9}$$

It can be easily shown that $\lambda_0 = 0$. Substituting (13.8) and (13.9) into (13.7), and comparing terms standing by the same powers of ε the following equations are obtained

$$\begin{gathered}
\varepsilon : \alpha_1\mu_1 + a_0 = 0, \\
\varepsilon^2 : \frac{1}{2}\alpha_1\mu_1^2 + a_1\mu_1 + \frac{1}{2}b_0 + \alpha_1\mu_2 = 0, \\
\varepsilon^3 : \alpha_0\mu_3 + \frac{1}{2}\alpha_2\mu_1\mu_2 + \frac{1}{6}\alpha_3\mu_1^3 + a_1\mu_2 + \frac{1}{2}a_2\mu_1^2 + \frac{1}{2}b_1\mu_1 + \frac{1}{6}c_0 = 0, \\
\ldots
\end{gathered} \tag{13.10}$$

which define $\mu_1, \mu_2, \mu_3, \ldots$ Hence a solution in the neighbourhood of (λ_0, x_0) has the following parameterized form

$$\begin{gathered}
x - x_0 = \varepsilon, \\
\lambda - \lambda_0 = \lambda_1\varepsilon + \lambda_2\varepsilon^2 + O(\varepsilon^3).
\end{gathered} \tag{13.11}$$

Note that if $\alpha_1 = F_\lambda(\lambda_0, x_0) = 0$, then one should use another parametrization, i.e. $x - x_0 = \psi(\varepsilon)$, $\lambda - \lambda_0 = \varepsilon$. Note also that if (λ_0, x_0) is singular then $\alpha_1 = a_0 = 0$ and we get

$$\alpha_2\mu_1^2 + 2a_1\mu_1 + 2b_0 = 0. \tag{13.12}$$

Therefore, if

(i) $a_1^2 > 2b_0\alpha_2$, then we have two distinct roots for μ;
(ii) $a_1^2 = 2b_0\alpha_2$, then we have double real solution (two branches of solution are tangent);
(iii) $a_1^2 < 2b_0\alpha_2$, then the roots are complex (the point (λ_0, x_0) is singular).

If $b_0 = a_1 = \alpha_2 = 0$, then (λ_0, x_0) is the triple point and first non-trivial algebraic equation is defined by the terms standing by ε^3. Many other examples are given in the mentioned monograph [144].

When various branches of solutions are found, the next step is focused on analysis of their stability. Consider one-dimensional problem governed by the equations

$$\begin{gathered}
\dot{x} = F(\lambda, x), \\
\dot{\nu} = F_\lambda(\lambda, x)\nu,
\end{gathered} \tag{13.13}$$

where the second equation governs behaviour of perturbations related to a being investigated singular points (equilibria). The discussed earlier Lyapunov's theorems can be used to estimate stability. Since we deal with one-dimensional case, then $F_\lambda(\lambda, x)$ defines the characteristic exponent of (13.13). If $\sigma = F_\lambda(\lambda, x)$ is negative, then a constant solution x of the original nonlinear differential equation is stable.

Observe that during stability investigation in the neighbourhood of the point (λ_0, x_0) we deal with the functions:

(i) $\sigma = \sigma(\lambda) = F_x(\lambda, x(\lambda))$ if a being investigated branch has the form $x = x(\lambda)$;
(ii) $\sigma = \sigma(\varepsilon) = F_x(\lambda(\varepsilon), x(\varepsilon))$ if a being investigated branch is parameterized by the equations $x - x_0 = \varepsilon$, $\lambda - \lambda_0 = \varphi(\varepsilon)$.

We give two examples studied in monograph [144].

Example 13.1. Consider the first-order differential equation with the right-hand side $F(\lambda, x) = -1-2\lambda+2\lambda x+\lambda^2+3x^2-2x^3$. Display existence and classification of singular points and build the corresponding bifurcation diagram.

Following the steps described earlier we obtain

$$F_x = 2\lambda + 6x - 6x^2,$$
$$F_\lambda = -2 + 2\lambda + 2x.$$

Solving two equations $F_x = 0$ and $F_\lambda = 0$, we obtain (0,1) as the singular point, which is doubled ($F_x(0, 1) = 0$, $F_{xx}(0, 1) \neq 0$). Introducing the parametrization

$$\varepsilon = x - 1,$$
$$\lambda = \mu_1\varepsilon + \mu_2\varepsilon^2 + O(\varepsilon^3),$$

we obtain:

$$\varepsilon^2: \quad \mu_1^2 + 2\mu_1 - 3 = 0$$
$$\varepsilon^3: \quad \mu_2 + \mu_1\mu_2 - 1 = 0.$$

Solving above algebraic equations we get: $\mu_{11} = 1$, $\mu_{12} = -3$, $\mu_{21} = 0,5$, $\mu_{22} = -0,5$. Hence, the following branches of solutions are found:

$$x = \varepsilon,$$
$$\lambda_1(\varepsilon) = 2\varepsilon - \varepsilon^2 + O(\varepsilon^3).$$

and

$$x = \varepsilon,$$
$$\lambda_2(\varepsilon) = -\varepsilon + O(\varepsilon^3).$$

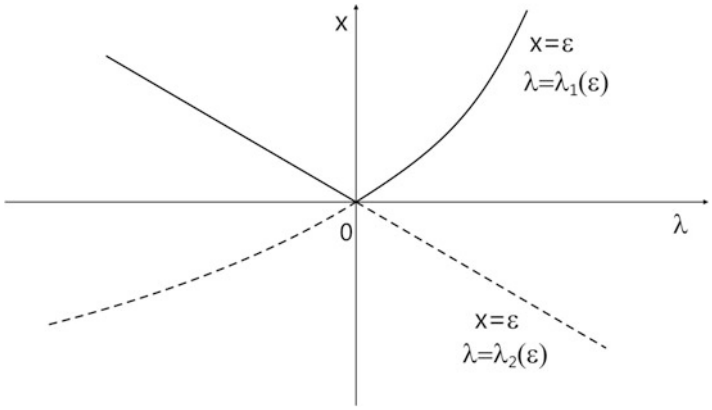

Fig. 13.7 Stable (*solid line*) and unstable (*dashed line*) branches of solutions in a vicinity of (0,0)

Stability of the obtained branches are defined by the exponents

$$\sigma_1(\varepsilon) = F_x[\lambda_1(\varepsilon), \varepsilon] = -6\varepsilon + O(\varepsilon^2),$$
$$\sigma_2(\varepsilon) = F_\lambda[\lambda_2(\varepsilon), \varepsilon] = -3\varepsilon + O(\varepsilon^2).$$

The corresponding bifurcation diagram is reported in Fig. 13.7. For $\varepsilon > 0$ ($\varepsilon < 0$) we have stable (unstable) branches.

□

Example 13.2. Consider a vertical slim rod of length l and a buckling caused by its gravity.

The equilibrium conditions of the rod element are:

(i) $\rho A\ddot{w}dx = dN\sin\alpha + dT\cos\alpha$ (transversal motion);
(ii) $dN\cos\alpha = qdx + dT\sin\alpha$ (longitudinal static condition);
(iii) $\frac{dM}{dx} = T$ (static condition),

where: ρ is the material density; A is the area of rod cross section; N is the normal force; T is the transversal force; M is the bending moment; α defines buckling angle and $(\cdot) = d/dt$.

From (iii), taking into account (i) and (ii), we get:

$$\rho\frac{Ad^2\ddot{w}}{dt^2} = \frac{\partial^2 M}{\partial x^2} + q\tan\alpha,$$

where

$$\tan\alpha = \frac{\partial w}{\partial x}, \quad \sqrt{1 + (\frac{dw}{dx})^2} = \frac{1}{\cos\alpha}.$$

The bending moment and a rod curvature are linked via relation

$$M = -EI\left(1 + \frac{dw}{dx}\right)^{-\frac{3}{2}},$$

where EI denotes the rod stiffness. Since we are going to consider rather large rod deflections then we include two nonlinear terms of the Taylor series of $M(w)$, and hence

$$M = -EI\frac{\partial^2 w}{\partial x^2}\left[1 - \frac{3}{2}\left(\frac{\partial w}{\partial x}\right)^2 + \frac{8}{15}\left(\frac{\partial w}{\partial x}\right)^4\right].$$

In addition, we approximate $(\cos\alpha)^{-1}$ by

$$\frac{1}{\cos\alpha} = 1 + \frac{1}{2}\left(\frac{\partial w}{\partial x}\right)^2.$$

Taking into account the above relations we obtain the partial differential equation governing slim vertical rod dynamics

$$\frac{d^2 w}{dt^2} = g\frac{\partial w}{\partial x} - \frac{EI}{\rho A}\left[\frac{\partial^4 w}{\partial x^4}\left(1 - \left(\frac{\partial w}{\partial x}\right)^2 + \frac{9}{8}\left(\frac{\partial w}{\partial x}\right)^4\right) - 9\frac{\partial w}{\partial x}\frac{\partial^2 w}{\partial x^2}\frac{\partial^3 w}{\partial x^3}\right.$$
$$\left. + - 3\frac{\partial^2 w}{\partial x^2} + 18\left(\frac{\partial w}{\partial x}\right)^3\frac{\partial^2 w}{\partial x^2}\frac{\partial^3 w}{\partial x^3} + 21\left(\frac{\partial w}{\partial x}\right)^2\left(\frac{\partial^2 w}{\partial x^2}\right)\right].$$

The boundary conditions for $w(x,t)$ include:

(a) geometrical

$$w(0,t) = 0, \quad \frac{dw}{dx}(0,t) = 0;$$

(b) approximate mechanical

$$\frac{d^2 w}{dx^2}(l,t) = 0, \quad \frac{d^3 w}{dx^3}(l,t) = 0.$$

In order to obtain an ordinary differential equation we separate the variables

$$w(x,t) = u(t)h(x).$$

Taking $h(x)$ as the fourth-order polynomial, and after orthogonalization procedure, we get

$$\ddot{u} = \left(\frac{A}{\lambda} - \frac{B}{\lambda^4}\right) u + \frac{C}{\lambda^6} u^3 - \frac{D}{\lambda^8} u^5,$$

where A, B, C, D are passive parameters, and $\lambda = l$ is the active parameter. Note that although we have second-order differential equation, we are going to investigate equilibria which are governed by

$$F(\lambda, u) = \left(\frac{A}{\lambda} - \frac{B}{\lambda^4}\right) u + \frac{C}{\lambda^6} u^3 - \frac{D}{\lambda^8} u^5 = 0$$

in a way similar to that of first-order differential equation. The trivial solution $u = 0$ corresponds to a straight form of the rod. The singular points are defined by

$$F_u(\lambda, u) = \frac{A}{\lambda} - \frac{B}{\lambda^4} + \frac{3C}{\lambda^6} u^2 - \frac{D}{\lambda^8} u^4 = 0,$$
$$F_\lambda(\lambda, u) = \left(-\frac{A}{\lambda^4} + \frac{4B}{\lambda^5}\right) u - \frac{2C}{\lambda^7} u^3 + \frac{4D}{\lambda^9} u^5 = 0.$$

For $u = 0$ from $F_\lambda = 0$ we get $\lambda_0 = \left(\frac{B}{A}\right)^{\frac{1}{3}}$. The point $(\lambda_0, u_0) = (\lambda_0, 0)$ is the singular point. Because $F_{\lambda u}(\lambda_0, 0) \neq 0$ than this is second-order singular point. The horizontal line $u = 0$ is one of the solutions crossing by this singular point. The second branch can be parameterized in the following way

$$u = \varepsilon,$$
$$\lambda - \lambda_0 = \mu_1 \varepsilon + \mu_2 \varepsilon^2 + \mu_3 \varepsilon^3 + \mu_4 \varepsilon^4 + O(\varepsilon^5).$$

The being sought numbers μ_1, μ_2, μ_3 and μ_4 are found from the equations:

$$\varepsilon: \; a_1 \mu_1 + \frac{1}{2} b_0 = 0;$$

(where $a_1 = F_{\lambda u}(\lambda_0, 0) = \frac{3A}{\lambda_0^2} > 0$, $b_0 = F_{uu}(\lambda_0, 0) = 0$ and hence $\mu_1 = 0$)

$$\varepsilon^2: \; a_1 \mu_2 + \frac{1}{6} c_0 = 0;$$

(where $c_0 = F_{uuu}(\lambda_0, 0) = \frac{6C}{\lambda_0^6} > 0$, and hence $\lambda_2 = -\frac{C}{3A\lambda_0^4} < 0$; it can be easy checked that also $\lambda_3 = 0$)

$$\varepsilon^4: \; a_1 \mu_4 + \frac{1}{2} a_2 \mu_2^2 + \frac{1}{6} c_1 \mu_2 + \frac{1}{5!} c_0 = 0;$$

(where $a_2 = F_{\lambda\lambda u}(\lambda_0, 0) = -\frac{18A^2}{B} < 0$, $c_1 = F_{\lambda uuu}(\lambda_0, 0) = \frac{36C}{\lambda_0^3} > 0$, $c_0 = F_{uuuuu}(\lambda_0, 0) = -\frac{5D}{\lambda_0^8} < 0$.) In result, we have found the following parameterized branches of non-trivial solution

$$u = \varepsilon$$
$$\lambda - \lambda_0 = \mu_2\varepsilon^2 + \mu_4\varepsilon^4 + O(\varepsilon^6),$$

where $\lambda_2 < 0$ and $\lambda_4 > 0$. Now let us investigate stability. In a case of the trivial solution

$$\sigma_1 = F_u(\lambda, 0) = \frac{A}{\lambda}\left(1 - \frac{\lambda_0^3}{\lambda^3}\right).$$

Hence $\sigma_1 > 0$, ($\sigma_1 < 0$) when $\lambda > \lambda_0$ ($\lambda < \lambda_0$). In the case of the second branch we have

$$\sigma_2(\varepsilon) = F_u\left(\lambda(\varepsilon), \varepsilon\right) = \frac{A}{\lambda(\varepsilon)} - \frac{B}{\lambda^4(\varepsilon)} - \frac{3C}{\lambda^6(\varepsilon)}\varepsilon^2 + \frac{5D}{\lambda^8(\varepsilon)}\varepsilon^4,$$

and consequently

$$\sigma_2(0) = 0; \quad \frac{d\sigma_2}{d\varepsilon}(0) = 0, \quad \frac{d^2\sigma_2}{d\varepsilon^2}(0) = -\frac{6C}{\lambda_0^6} < 0.$$

The exponent σ_2 can be approximated by

$$\sigma_2(\varepsilon) = -\frac{3C}{\lambda_0^6}\varepsilon^2 + O(\varepsilon^3).$$

In the extremum of this branch, which is equal to $\varepsilon_{ex} = \pm\left(\frac{\mu_2}{\mu_4}\right)^{\frac{1}{2}}$, a change of stability occurs.

The results are shown in Fig. 13.8, where the hysteresis loop $E1, E2, E3, E4$ is remarkable. □

13.2.2 Two-Dimensional Vector Fields

Consider how two nonlinear algebraic equations with one parameter λ of the form

$$F_i\left(x_1, x_2, \lambda\right) = 0, \quad i = 1, 2 \tag{13.14}$$

and $x_{10}, x_{20}, \lambda_0$ is a solution of (13.14).

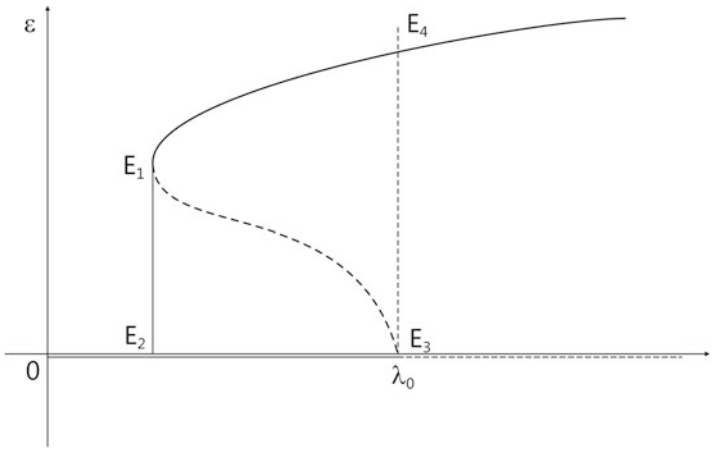

Fig. 13.8 Bifurcation diagram of a slim rod buckling

Theorem 13.3 (Implicit Function Theorem). *If the Jacobian associated with (13.14)* $\frac{\partial F_i}{\partial x_i}(x_{10}, x_{20}, \lambda_0) \neq 0$ *then there is a neighbourhood of the point* $(x_{10}, x_{20}, \lambda_0)$*, where the curve defined by (13.14), is unique, i.e. there exist such functions* $x_i(\lambda)$ *that*

$$F_i\left[x_1(\lambda), x_2(\lambda), \lambda\right] = 0,\ i = 1, 2. \tag{13.15}$$

In words, if the associated Jacobian with the investigated point differs from zero then there are no other solutions in a neighbourhood of the point $(x_{10}, x_{20}, \lambda_0)$. A necessary condition for bifurcation is defined by $\frac{\partial f_i}{\partial x_i}(x_{10}, x_{20}, \lambda_0) = 0,\ i = 1, 2$.

Now we are going to describe briefly a construction of a bifurcation solution of the system (13.14). We consider a trivial case, i.e. we assume that $x_{10} = x_{20} = 0$ is the solution of Eq. (13.14), and $\lambda = 0$ corresponds to a critical state of the system.

Since

$$F_i\,(0, 0, \lambda) = 0, \quad i = 1, 2, \tag{13.16}$$

hence

$$\begin{aligned} F_1\,(x_1, x_2, \lambda) &= a\,(\lambda)\,x_1 + b\,(\lambda)\,x_2 + \alpha_1\,(\lambda)\,x_1^2 + 2\beta_1\,(\lambda)\,x_1 x_2 \\ &\quad + \gamma\,(\lambda)\,x_2^2 + O\left(\|x\|^3\right), \\ F_2\,(x_1, x_2, \lambda) &= c\,(\lambda)\,x_1 + d\,(\lambda)\,x_2 + \alpha_2\,(\lambda)\,x_1^2 + 2\beta_2\,(\lambda)\,x_1 x_2 \\ &\quad + \gamma\,(\lambda)\,x_2^2 + O\left(\|x\|^3\right), \end{aligned} \tag{13.17}$$

where $a, b, c, d, \alpha_i, \beta_i$ and γ_i (i=1, 2) depend on the parameter λ and $\|\cdot\|$ denotes a norm in two-dimensional Euclidian space. The associated variational (perturbational) equations have the form

$$\begin{bmatrix} \dot{x}_1 \\ \dot{x}_2 \end{bmatrix} = \left(\begin{bmatrix} a_0 & b_0 \\ c_0 & d_0 \end{bmatrix} + \begin{bmatrix} a_1 & b_1 \\ c_1 & d_1 \end{bmatrix} \lambda + O\left(\lambda^2\right) \right) \begin{bmatrix} x_1 \\ x_2 \end{bmatrix}. \tag{13.18}$$

A bifurcation condition leads to the equation

$$\det [A_0] = \begin{vmatrix} a_0 & b_0 \\ c_0 & d_0 \end{vmatrix} = 0. \tag{13.19}$$

It is clear that $\det [A_0] = 0$, if at least one of the eigenvalues of the matrix A_0 is equal to zero. Knowing that $(0, 0, 0)$ is the bifurcation point one needs to find a number of bifurcating solutions (from this point) occurring in a small vicinity of $\lambda = 0$. Taking into account the small increments of the variables and functions in (13.16) and dividing the obtained linear equations by $d\lambda$ one obtains

$$\begin{aligned} \frac{dF_1}{d\lambda} &= a_0 \frac{dx_1}{d\lambda} + b_0 \frac{dx_2}{d\lambda}, \\ \frac{dF_2}{d\lambda} &= c_0 \frac{dx_1}{d\lambda} + d_0 \frac{dx_2}{d\lambda}. \end{aligned} \tag{13.20}$$

This linear approximation cannot be used to find uniquely higher order derivatives. One should include the nonlinear terms. For the case, when only quadratic terms are taken into account, we get

$$\begin{aligned} a_0 \frac{dx_1}{d\lambda} + b_0 \frac{dx_2}{d\lambda} + \alpha_{10} \left(\frac{dx_1}{d\lambda} \right)^2 + 2\beta_{10} \frac{dx_1}{d\lambda} \frac{dx_2}{d\lambda} + \gamma_{10} \left(\frac{dx_2}{d\lambda} \right)^2 = 0, \\ c_0 \frac{dx_1}{d\lambda} + d_0 \frac{dx_2}{d\lambda} + \alpha_{20} \left(\frac{dx_1}{d\lambda} \right)^2 + 2\beta_{20} \frac{dx_1}{d\lambda} \frac{dx_2}{d\lambda} + \gamma_{20} \left(\frac{dx_2}{d\lambda} \right)^2 = 0. \end{aligned} \tag{13.21}$$

A number of bifurcating solutions is defined by a number of intersection points of two conical curves represented by Eq. (13.21). One can have 1, 2 or 3 solutions, in spite of the trivial one.

In general we have three different cases to be considered in two-dimensional vector fields:

(i) one eigenvalue is equal to zero;
(ii) two eigenvalues are zero with degeneracy order 1;
(iii) two eigenvalues are zero with a degeneracy order 2.

We consider only the case (i) and we follow the steps studied in the monograph [144].

Let us introduce the following parameterization

$$x_1 = \varepsilon,\ x_2 = \varepsilon y\left(\varepsilon\right),\ \lambda = \varepsilon\mu\left(\varepsilon\right), \tag{13.22}$$

or

$$x_1 = \varepsilon x\left(\varepsilon\right),\ x_2 = \varepsilon,\ \lambda = \varepsilon\mu\left(\varepsilon\right). \tag{13.23}$$

The functions $x\left(\varepsilon\right)$, $y\left(\varepsilon\right)$ and $\lambda\left(\varepsilon\right)$ are polynomials and can be found in a way described earlier. Using parameterization (13.22) the being analysed Eq. (13.14) can be presented in the form

$$\varepsilon g_i\left[\mu\left(\varepsilon\right), y\left(\varepsilon\right), \varepsilon\right] = 0, \quad i = 1, 2, \tag{13.24}$$

where

$$\begin{aligned} g_1 &= a_0 + a_1\varepsilon\mu + \left(b_0 + b_1\varepsilon\mu\right) y + \alpha_1\varepsilon + 2\beta_1\varepsilon y + \gamma_1\varepsilon y^2 + O\left(\varepsilon^2\right), \\ g_2 &= c_0 + c_1\varepsilon\mu + \left(d_0 + d_1\varepsilon\mu\right) y + \alpha_2\varepsilon + 2\beta_2\varepsilon y + \gamma_2\varepsilon y^2 + O\left(\varepsilon^2\right). \end{aligned} \tag{13.25}$$

In fact, we are going to find the functions $y\left(\varepsilon\right)$ and $\mu\left(\varepsilon\right)$ which satisfy the equations

$$\begin{aligned} a_0 + b_0 y + \varepsilon\left[\left(a_1 + b_1 y\right)\mu + \alpha_1 + 2\beta_1 y + \gamma_1 y^2\right] + O\left(\varepsilon^2\right) = 0, \\ c_0 + d_0 y + \varepsilon\left[\left(c_1 + d_1 y\right)\mu + \alpha_2 + 2\beta_2 y + \gamma_2 y^2\right] + O\left(\varepsilon^2\right) = 0. \end{aligned} \tag{13.26}$$

For $\varepsilon = 0$ we obtain two dependent equations and hence $y_0 = y\left(0\right) = -\frac{a_0}{b_0} = -\frac{c_0}{d_0}$ for $b_0 \neq 0$ or $d_0 \neq 0$.

In the case $b_0 = d_0 = 0$ one needs to apply the following parametrization $x_1 = \varepsilon x\left(\varepsilon\right), x_2 = \varepsilon, \lambda = \varepsilon\mu\left(\varepsilon\right)$. In a similar way, one obtains $x_0 = x\left(0\right) = -\frac{b_0}{a_0} = -\frac{d_0}{c_0}$ for either $a_0 \neq 0$ or $c_0 \neq 0$. Let

$$y\left(\varepsilon\right) = y_0 + \varepsilon\tilde{y}\left(\varepsilon\right) \tag{13.27}$$

Substituting (13.27) into (13.26) we get

$$\varepsilon h_i\left(\lambda, \tilde{y}, \varepsilon\right) = 0, \quad i = 1, 2, \tag{13.28}$$

where

$$\begin{aligned} h_1 &= b_0\tilde{y} + \mu\left(a_1 + b_1 y\right) + \alpha_1 + 2\beta_1 y_0 + \gamma_1 y_0^2 + O\left(\varepsilon\right), \\ h_2 &= d_0\tilde{y} + \mu\left(c_1 + d_1 y\right) + \alpha_2 + 2\beta_2 y_0 + \gamma_2 y_0^2 + O\left(\varepsilon\right). \end{aligned} \tag{13.29}$$

Since for $\varepsilon = 0$ we have $h_i = 0$, hence we get two linear equations of the form

$$\begin{aligned} b_0\tilde{y_0} + \mu_0 (a_1 + b_1 y_0) + \alpha_{10} + 2\beta_{10} y_0 + \gamma_{10} y_0^2 = 0, \\ d_0\tilde{y_0} + \mu_0 (c_1 + d_1 y_0) + \alpha_{20} + 2\beta_{20} y_0 + \gamma_{20} y_0^2 = 0, \end{aligned} \tag{13.30}$$

which serve to find $(y_0, \tilde{\mu_0})$. The first (linear) approximation to the being sought bifurcated solutions has the form

$$x_1 = \varepsilon, x_2 = \varepsilon y_0, \lambda = \varepsilon\mu_0. \tag{13.31}$$

Note that the solution $(\tilde{y_0}, \mu_0)$ is the only one, and $\varepsilon = \sqrt{x_1^2 + \left(\frac{x_2}{y_0}\right)^2}$ measures a distance between the bifurcational and trivial solutions. One can include more terms in order to get nonlinear functions $\varepsilon(\lambda)$ and $\mu(\varepsilon)$. The associated linear variational equation defines a local phase flow in a vicinity of a being investigated non-trivial solution. Introducing the local variables $v_1 = u_1 - \varepsilon$ and $v_2 = u_2 - \varepsilon y_0$ one obtains

$$\begin{bmatrix} \dot{v}_1 \\ \dot{v}_2 \end{bmatrix} = \begin{bmatrix} a_0 + \varepsilon (\lambda_0 a_1 + 2\alpha_{10} + 2\beta_{10}) & b_0 + \varepsilon (\lambda_0 b_1 + 2\beta_{10} + 2\gamma_{10}) \\ c_0 + \varepsilon (\lambda_0 c_1 + 2\alpha_{20} + 2\beta_{20}) & d_0 + \varepsilon (\lambda_0 d_1 + 2\beta_{20} + 2\gamma_{20}) \end{bmatrix} \begin{bmatrix} v_1 \\ v_2 \end{bmatrix} \tag{13.32}$$

The bifurcating solution (13.31) is unstable in Lyapunov sense if at least one eigenvalue $\sigma_i(\varepsilon), i = 1, 2$ has a positive real part. For a case $a_0 = b_0 = c_0 = 0$ and $d_0 < 0$ from (13.32) one gets

$$\begin{bmatrix} \dot{v}_1 \\ \dot{v}_2 \end{bmatrix} = \begin{bmatrix} c_1\varepsilon & c_2\varepsilon \\ c_3\varepsilon & d_0 + c_4\varepsilon \end{bmatrix} \begin{bmatrix} v_1 \\ v_2 \end{bmatrix}, \tag{13.33}$$

where c_i are real values. The associated eigenvalues are easily found

$$\sigma_{1,2}(\varepsilon) = \frac{d_0 + (c_1 + c_2)\varepsilon}{2} \pm \frac{1}{2}\sqrt{d_0^2 + 2d_0 (c_4 - c_1)\varepsilon}, \tag{13.34}$$

and for enough small ε they can be represented by their linear part only

$$\sigma_1(\varepsilon) = c_1\varepsilon, \sigma_2(\varepsilon) = d_0 + c_4\varepsilon. \tag{13.35}$$

The corresponding bifurcational diagram is shown in Fig. 13.9. Unstable solutions are marked by a dashed line.

Example 13.3. Display a bifurcation diagram and investigate stability of all branches of solutions occurred in the system

$$\begin{aligned} \dot{x_1} &= px_1 - px_2 - x_1^2 + x_2^2 + x_1^3, \\ \dot{x_2} &= px_2 + x_1x_2 + 2x_1^3. \end{aligned}$$

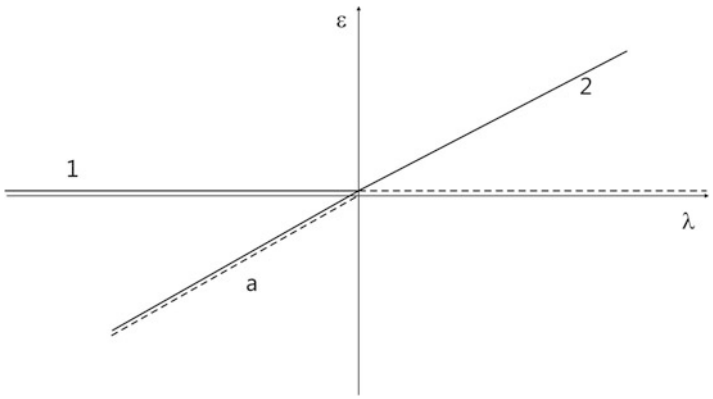

Fig. 13.9 Bifurcational diagram corresponding to simple zero eigenvalue (*1* primary (trivial) solution; *2* secondary (bifurcated) solution)

First we observe that a matrix associated with the origin does not have the terms independent on p, hence $A_0 = 0$. We have double zero eigenvalue for $p = 0$, with the Riesz index $\nu = 1$ and degeneracy order 2. The eigenvalues of the matrix A are $\sigma_{1,2} = p$.

We introduce the following parametrization

$$\begin{aligned} x_1 &= \varepsilon, \\ x_2 &= \varepsilon y_0 + \varepsilon^2 y_1 + O\left(\varepsilon^3\right), \\ p &= \varepsilon \mu_0 + \varepsilon^2 \mu_1 + O\left(\varepsilon^3\right), \end{aligned}$$

and we substitute the above equations to the analysed differential equations. The following algebraic equations are obtained

$$\begin{aligned} \varepsilon^2 : \; & \mu_0 - \mu_0 y_0 - 1 + y_0^2 = 0, \\ & (\mu_0 + 1)\, y_0 = 0; \\ \varepsilon^3 : \; & \mu_1 (1 - y_0) + y_1 (2y - \mu_0) = -1, \\ & \mu_1 y_0 + y_1 (1 + \mu_0) = -2. \end{aligned} \qquad (*)$$

Their solutions are

$$\begin{aligned} y_0^{(1)} = 0, \quad y_0^{(2)} = 1, \quad y_0^{(3)} = -2, \\ \mu_0^{(1)} = 1, \quad \mu_0^{(2)} = -1, \quad \mu_0^{(3)} = -1. \end{aligned}$$

Since for each of three above pairs (y_0, μ_0) the main determinant of $(*)$ is not equal to zero, there are three pairs of solutions $\left(y_1^{(k)}, \mu_1^{(k)}\right)$ corresponding to three pairs $\left(y_0^{(k)}, \mu_0^{(k)}\right)$ for $k = 1, 2, 3$:

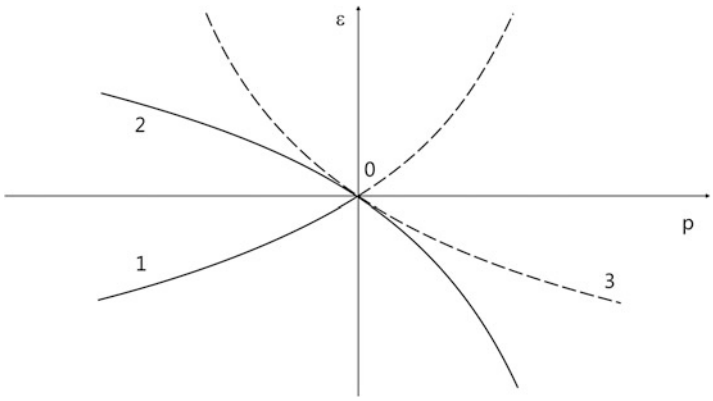

Fig. 13.10 Four branches of solutions (*dashed curves* correspond to unstable ones)

$$y_1^{(1)} = -1, \quad y_1^{(2)} = -\frac{1}{3}, \quad y_1^{(3)} = \frac{4}{3},$$
$$\mu_1^{(1)} = -1, \quad \mu_1^{(2)} = -2, \quad \mu_1^{(3)} = 1.$$

Therefore we have the following three branches of bifurcating solutions (see Fig. 13.10)

$$\begin{array}{ccc} x_1^{(1)} = \varepsilon, & x_1^{(2)} = \varepsilon, & x_1^{(3)} = \varepsilon, \\ x_2^{(1)} = -\varepsilon^2 + O\left(\varepsilon^3\right), & x_2^{(2)} = \varepsilon - \frac{1}{3}\varepsilon^3 + O\left(\varepsilon^2\right), & x_2^{(3)} = -2\varepsilon - \frac{4}{3}\varepsilon^2 + O\left(\varepsilon^2\right), \\ p^{(1)} = \varepsilon - \varepsilon^2 + O\left(\varepsilon^3\right), & p^{(2)} = -\varepsilon - 2\varepsilon^2, & p^{(3)} = -\varepsilon + \varepsilon^2 + O\left(\varepsilon^3\right). \end{array}$$

A stability of each bifurcated solutions depends on the eigenvalues of the matrix calculated in the point $x_1 = \varepsilon$, $x_2 = \varepsilon y_0$, $p = \varepsilon\mu_0$

$$B(\varepsilon) = \begin{bmatrix} \frac{\partial F_1}{\partial x_1} & \frac{\partial F_1}{\partial x_2} \\ \frac{\delta F_2}{\partial x_1} & \frac{\partial F_2}{\partial x_2} \end{bmatrix} = \varepsilon^2 \begin{bmatrix} \mu_0 - 2 & 2y_0 - \mu_0 \\ y_0 & 1 + \mu_0 \end{bmatrix} = \varepsilon_2 B_0.$$

Now, taking three pairs (y_0, μ_0) we obtain

$$B_0^{(1)} = \begin{bmatrix} -1 & -1 \\ 0 & 2 \end{bmatrix}, \; B_0^{(2)} = \begin{bmatrix} -3 & 3 \\ 1 & 0 \end{bmatrix}, \; B_0^{(3)} = \begin{bmatrix} -3 & -3 \\ -2 & 0 \end{bmatrix},$$

and the corresponding eigenvalues read

$$\sigma_{01}^{(1)} = -1, \; \sigma_{02}^{(1)} = 2, \; \sigma_{01,2}^{(2)} = -\tfrac{3}{2} \pm \tfrac{1}{2}\sqrt{21}, \; \sigma_{01,2}^{(3)} = -\tfrac{3}{2} \pm \tfrac{1}{2}\sqrt{33}.$$

□

All of the so far presented examples are taken from the monograph [144].

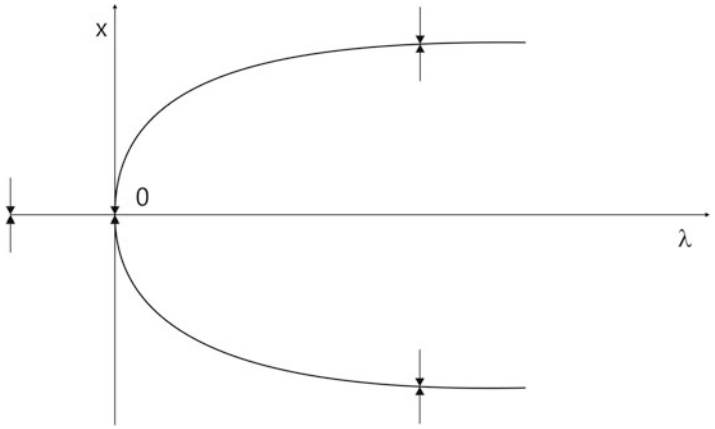

Fig. 13.11 Saddle-node bifurcation

13.2.3 Local Bifurcation of Hyperbolic Fixed Points

In the previous sections we have shown a general approach to analyse bifurcation appeared in one- and two-dimensional vector fields. Here we present local bifurcations of hyperbolic fixed points. A reader can easily apply the described earlier method to construct the corresponding bifurcation diagrams.

(i) *A saddle-node bifurcation*

This bifurcation is governed by the equation

$$\dot{x} = \lambda - x^2 \tag{13.36}$$

with the corresponding bifurcation diagram shown in Fig. 13.11.

(ii) A *transcritical bifurcation.*

This bifurcation is characterized by vector field

$$\dot{x} = \lambda x - x^2 \tag{13.37}$$

and its associated bifurcation diagram is shown in Fig. 13.12.

(iii) A *pitchfork bifurcation.*

This bifurcation occurs in the one-dimensional system with a cubic type nonliberality and is governed by the vector field

$$\dot{x} = \lambda x - x^3. \tag{13.38}$$

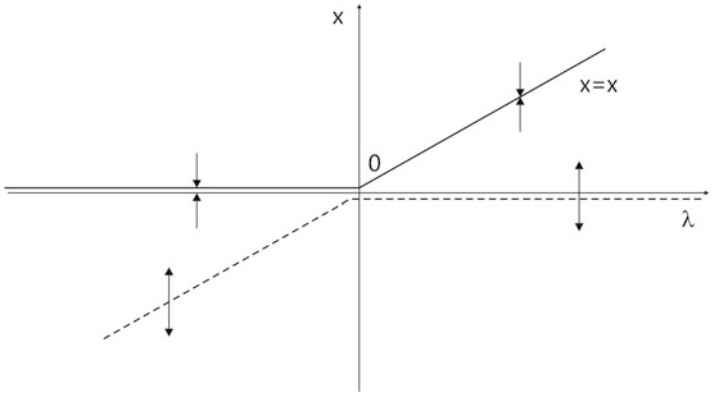

Fig. 13.12 A transcritical bifurcation

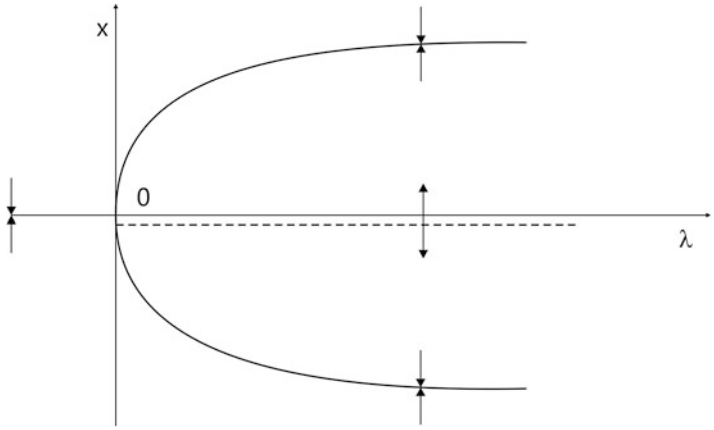

Fig. 13.13 A pitchfork bifurcation

The bifurcation diagram is shown in Fig. 13.13.

Note that for $\lambda < 0$ we have one branch of solutions, whereas for $\lambda > 0$ there are three branches of solution (two stable and one unstable).

There is another important question related to the so-called normal forms of the classical local bifurcations. In words, having a Taylor expansion around a trivial non-hyperbolic fixed point of a general parameter family of one-dimensional vector fields one can characterize the different geometry of the curves passing through origin by an appropriate truncation of the series. For example by adding the signs "$\pm$" instead of the sign before two terms on the right-hand side of (13.36), (13.37) and (13.38) we get the normal form of the mentioned local bifurcations.

13.2.4 Bifurcation of a Non-hyperbolic Fixed Point (Hopf Bifurcation)

The Hopf bifurcation plays a role of a door between static and dynamics and is very important in engineering. In spite of the original work of [124] a problem when a previously stable equilibrium becomes unstable and in a critical bifurcation point periodic orbit appear has been analysed also by Andronov et al. in the thirtieth (see [8,43]). Then in seventieth this central problem for dynamics has been reconsidered by many researchers like Chow and Mallet-Paret [64], Crandall and Rabinowitz [73], Hale [112], Hale and Oliveria [113], Hassard et al. [115], Holmes [123], Marsden and McCracken [164], Golubitsky and Schaeffer [100], Golubistky et al. [101], and others [125]. Here we briefly follow the approach described by Hassard [115].

Consider the following differential equations

$$\dot{x} = F(p, x), \qquad x \in \mathbb{R}^n. \tag{13.39}$$

We assumed that p is the bifurcation parameter and for $p_{cr} = 0$ we have $F(p_{cr}, 0) = 0$. We say that the system (13.39) has a family of periodic solutions with the parameter $\varepsilon \in (0, \varepsilon_0)$, and the amplitude of periodic solutions tends to zero when the formally introduced parameter $\varepsilon \to 0$.

Theorem 13.4 (Hopf). *Given*

(i) $F(p, 0) = 0$ *for every* p *from an open interval including* $p = 0$ *and* $0 \in \mathbb{R}^n$ *is the isolated fixed point of (13.39);*

(ii) The function F *is analytical with regard to* p *and* x *in a certain neighbourhood of* $(0, 0) \in \mathbb{R}^n \times \mathbb{R}^1$*;*

(iii) The matrix $A(p)$ *of the linearized system in a vicinity of zero solution has a pair of conjugated eigenvalues* σ *and* $\bar{\sigma}$*, where*

$$\sigma(p) = \xi(p) + i\eta(p), \tag{13.40}$$

and

$$\xi(0) = 0, \qquad \frac{d\xi}{dp}(0) \neq 0, \qquad \eta(0) = \eta_0 > 0; \tag{13.41}$$

(iv) Other eigenvalues of the matrix $A(0)$ *possess negative real parts.*

Then the system (13.39) has a family of periodic solutions. In addition, there is a certain ε^H *and an analytical function*

$$p^H(\varepsilon) = \sum_{i=2}^{\infty} p_i \varepsilon^i, \qquad (0 < \varepsilon < \varepsilon^H), \tag{13.42}$$

such that for every $\varepsilon \in (0, \varepsilon^H)$ *the system (13.39) for* $p = p^H(\varepsilon)$ *has a periodic solution* $x_\varepsilon(t)$.

The period of periodic solution $x_\varepsilon(t)$ is the analytical function

$$T^H(\varepsilon) = \frac{2\pi}{\eta_0}(1 + \sum_{i=2}^{\infty} \tau_i \varepsilon^i), \qquad (0 < \varepsilon < \varepsilon^H). \tag{13.43}$$

For every $L > 2\pi/p_0$ there is a neighbourhood R of the point $x = 0$ ($x \in \mathbb{R}^n$) and an open interval J including 0, such that for every $p \in J$ the periodic solution to the system (13.39) which lie in R and have a period smaller then T^H are the members of the family $x_{\varepsilon(t)}$ for which $p^H(\varepsilon) = p, \varepsilon \in (0, \varepsilon^H)$. The solutions which differ by an initial phase and corresponding to the same $x_\varepsilon(t)$ cannot be distinguishable. If $p^H(\varepsilon)$ is not identically equal to zero, then a first nonzero coefficient p_i has an even index. There exists such $\varepsilon^1 \in (0, \varepsilon^H)$ that $p^H(\varepsilon)$ is either positive or negative for $\varepsilon \in (0, \varepsilon^1)$. Two Floquet exponents of the solution $x_\varepsilon(t)$ tend to zero for $\varepsilon \to 0$. One of them is identically equal to zero for $\varepsilon \in (0, \varepsilon^H)$, whereas second one

$$\sigma(\varepsilon) = \sum_{i=2}^{\infty} \sigma_i \varepsilon^i, \qquad 0 < \varepsilon < \varepsilon^H. \tag{13.44}$$

The periodic solution $x_\varepsilon(t)$ is orbitally stable (unstable) with the asymptotic phase, if $\sigma(\varepsilon) < 0 \quad (\sigma(\varepsilon) > 0)$.

The proof of the Hopf theorem is here omitted, but it can be found in the work of Marsden and McCracken [164]. Although the Hopf theorem in its source version is related to the systems with analytical right-hand sides, but the similar like theorems have been formulated later for the right-hand sides being differentiable (see [115]). We have used the same reference to formulate the Hopf theorem. The main idea of the proof is focused on reduction of initial n-dimensional system to two-dimensional Poincaré form with use of the central manifold theory. A construction of a bifurcated solution relies on application of the normal Poincaré form. Another alternative approach has been presented by Iooss and Joseph [127] (see also Kurnik [145]). We present the later one, since it seems to be more economical leading to estimate bifurcating solutions and their stability.

Assume that self-excited oscillations equation of a mechanical system with lumped parameters is governed by the equation

$$\dot{U} = F(\nu, U; Q), \tag{13.45}$$

where $U \in \mathbb{R}^n$ and $F : \mathbb{R}^n \times \mathbb{R}^n \to \mathbb{R}^n$, ν is the parameter governing self-excitation and further referred as the bifurcation parameter; Q is another parameter.

Assume that F is analytical with regard to U and ν in a vicinity of ν_{cr}. Let $U^* = U^*(\nu, Q)$ be a constant solution. Note that for each Q the constant solution depends on bifurcation parameter, and hence we have a family of constant solutions. On the other hand, for a given ν and Q, one may have many solutions $U_1^*, U_2^*, \ldots$.

Dealing with a Hopf bifurcation we consider one of the U_i^* solutions. The corresponding critical value of ν is found investigating stability of the being analysed constant solution $U^*(\nu, Q)$. Assuming that $A(\nu, Q)$ is the matrix corresponding to the linearized system, then the characteristic equation is

$$\det(A - \sigma I) = 0, \tag{13.46}$$

where I is the identity $n \times n$ matrix.

The critical point $\nu = \nu_{cr}(Q)$ is defined by $\mathrm{Re}\{\sigma_1(\nu_{cr}, Q)\} = 0$, where $\sigma_1 > \sigma_i$, $i = 2, \ldots, n$. Then the system (13.45) is transformed to its local form by introducing the variable $u = U - U^*(\nu, Q)$, and the parameter $\omega = \nu - \omega_{cr}$. Equation (13.45) is recast to the following form

$$\dot{u} = f(\omega, u), \tag{13.47}$$

where: $f(\omega, u) = F(\omega + \omega_{cr}, u + U^*; Q) - F(\omega + \omega_{cr}, U^*; Q)$, $Q, \omega \in \mathbb{R}^+, u, U^* \in \mathbb{R}^n$.

Observe that $f(\omega, 0) = 0$. The parameter Q will be further omitted to simplify our considerations. Therefore the problem is reduced to consideration of the following system

$$\dot{u} = A(\omega)u + N(\omega, u), \tag{13.48}$$

where $A(\omega, Q) = A(\omega)$, $A_{ij} = [\frac{\partial f_i}{\partial u_j}]_{u=0}$.

Let $\sigma_1(\omega), \ldots, \sigma_n(\omega)$ be the eigenvalues of $A(\omega)$. Claiming also that the assumptions of Hopf theorem are satisfied in a vicinity of the critical point:

$$\begin{gathered} \mathrm{Re}\,\sigma_1(0) = \xi(0) = 0, \\ \mathrm{Im}\,\sigma_2(0) = \eta(0) = \Omega_0, \\ \tfrac{d\xi}{d\omega}(0) \neq 0, \end{gathered} \tag{13.49}$$

where Ω_0 is the positive number and $\sigma_1, \sigma_2 = \bar{\sigma}_1$ are simple eigenvalues.

Let q and q^* be the eigenvectors of the matrix $A(\omega)$ and $A^*(\omega) = A^T(\omega)$, respectively. They are associated with the imaginary eigenvalues in the critical point. These are found from the equations

$$\begin{aligned} (A(0) - \sigma_1(0)I)q &= 0, \\ (A^T(0) - \bar{\sigma}_1(0)I)q^* &= 0. \end{aligned} \tag{13.50}$$

The required uniqueness is achieved by introduction of the normalization procedure

$$\langle q, q^* \rangle = 1, \tag{13.51}$$

where $\langle q, q^* \rangle = \sum_{i=1}^{n} a_i \bar{b}_i$ is the Hermitean scalar product in complex n-dimensional Euclidean space and the vectors q and $\bar{q}^*$ are orthogonal, i.e.

$$\langle q, \bar{q}^* \rangle = \sum_{i=1}^{n} q_i q_i^* = 0. \tag{13.52}$$

They are linearly independent and they will play a role of skeleton of being sought periodic solutions. The vector q^* will be used during implementation of the orthogonal condition within the Fredholm alternative.

The being sought bifurcated solution has the form

$$u(s, \varepsilon) = \sum_{i=1}^{\infty} \frac{1}{n!} u^{(n)}(s) \varepsilon^n, \tag{13.53}$$

where $s = \Omega(\varepsilon)t$. We take

$$\begin{aligned} \Omega(\varepsilon) &= \Omega_0 + \sum_{i=1}^{\infty} \frac{1}{n!} \varepsilon^n \Omega_n, \\ \omega(\varepsilon) &= \omega_{cr} + \sum_{i=1}^{\infty} \frac{1}{n!} \varepsilon^n \omega_n, \quad (\omega_{cr} = 0), \end{aligned} \tag{13.54}$$

where Ω is the frequency of the sought periodic solution; $\Omega_0 = \mathrm{Im}\,\sigma_1(0); \omega_n$ and Ω_n are the series terms; $u^{(n)}(s)$ is the series of $2\pi-$ periodic continuous and differentiable functions; ε is the parameter measuring the distance between a trivial, and periodic solutions in a sense of the applied norm.

Note that an existence of bifurcated solutions in the form (13.53) is guaranteed by Hopf theorem. Let $P_{2\pi}$ is the space of complex and $2\pi-$periodic functions, continuous and differentiable, where the following scalar product is defined

$$[a(s), b(s)] \stackrel{\mathrm{df}}{=} \frac{1}{2\pi} \int_0^{2\pi} < a(s), \bar{b}(s) > ds, \tag{13.55}$$

and we take the norm

$$\|a\| = \sqrt{[\bar{a}, a]}. \tag{13.56}$$

In addition, following Iooss and Joseph ([127]), we introduce the Maclaurin series of the function $f(u, t; \omega, p)$ with regard to u. Since $f(0, t; \omega, p) \equiv 0$, hence

$$f(u, t; \omega, p) = \sum_{i=1}^{\infty} \frac{1}{n!} f_{uu\ldots u}(\omega, p, t, 0|u|u| \ldots |u), \tag{13.57}$$

where $f_{uu\ldots u}(\omega, p, t, 0|u|u|\ldots|u)$ is nth-linear operator acting on the vector u in neighbourhood of $u = 0$.

In general, an nth-linear operator of the vector field $f(u, t, \omega, p)$ acting on the vectors $a_1, a_2, \ldots, a_n$ in an arbitrary point u_0 is defined by

$$f_{uu\ldots u}(\omega, p, t, u_0|a_1|a_2|\ldots|a_n) = \lim_{h_1,h_2,\ldots,h_n\to 0} \frac{\partial^{(n)} f(u_0+h_1a_1+\cdots+h_na_n, t; \omega, p)}{\partial h_1 \partial h_2 \ldots \partial h_n} \tag{13.58}$$

The right-hand side of (13.47) can be developed into the Maclaurin series

$$f(\omega, u) = \sum_{i=1}^{\infty} \frac{1}{n!} f_{uu\ldots u}(\omega, 0|u|u|\ldots|u). \tag{13.59}$$

On the other hand, each term of the series (13.59) is developed into the Maclaurin series with regard to ω:

$$\begin{aligned} f(\omega, u) &= f_u(0, 0|u) + f_{u\omega}(0, 0|u)\omega + \frac{1}{2!} f_{u\omega\omega}(0, 0|u)\omega^2 + \cdots \\ &\ldots + \frac{1}{2!}\left\{ f_{uu}(0, 0|u|u) + f_{uu\omega}(0, 0|u|u)\omega + \frac{1}{2!} f_{uu\omega\omega}(0, 0|u|u)\omega^2 + \cdots \right\} \\ &+ \frac{1}{3!}\left\{ f_{uuu}(0, 0|u|u|u) + f_{uuu\omega}(0, 0|u|u|u)\omega + \frac{1}{2!} f_{uuu\omega\omega}(0, 0|u|u|u)\omega^2 + \cdots \right\} + \cdots \end{aligned} \tag{13.60}$$

and hence

$$\begin{aligned} f(\omega, u) &= \sum_{i=1}^{\infty} \frac{\varepsilon^i}{i!} f_u(0, 0|u^{(i)}) \\ &+ \sum_{i=1}^{\infty}\sum_{j=1}^{\infty} \frac{\varepsilon^{i+j}}{i!j!} f_{u\omega}(0, 0|u^{(i)})\omega_j + \frac{1}{2!} f_{uu\omega}(0, 0|u^{(i)}|u^{(j)}) \\ &+ \sum_{i=1}^{\infty}\sum_{j=1}^{\infty}\sum_{k=1}^{\infty} \frac{\varepsilon^{i+j+k}}{i!j!k!}\{ f_{u\omega\omega}(0, 0|u^{(i)})\omega_j\omega_k + \frac{1}{2!} f_{uu\omega}(0, 0|u^{(i)}|u^{(j)})\omega_k \\ &+ \frac{1}{3!}\{ f_{uuu}(0, 0|u^{(i)}|u^{(j)}|u^{(k)})\} + \sum_{i=1}^{\infty}\sum_{j=1}^{\infty}\sum_{k=1}^{\infty}\sum_{l=1}^{\infty} \frac{\varepsilon^{i+j+k+l}}{i!j!k!l!}\{\ldots\} + \cdots \end{aligned} \tag{13.61}$$

The left-hand side of (13.47) has the form

$$\dot{u} = \Omega_0 \sum_{i=1}^{\infty} \frac{\varepsilon^i}{i!} \frac{du^{(i)}}{ds} + \sum_{i=1}^{\infty}\sum_{j=1}^{\infty} \frac{\varepsilon^{i+j}}{i!j!} \Omega_j \frac{du^{(i)}}{ds}. \tag{13.62}$$

Comparing the same terms by the same powers of ε in (13.61) and (13.62) we get

$$
\begin{aligned}
&-\Omega_0 \frac{du^{(1)}}{ds} + f_u(0,0|u^{(1)}) = 0 \quad (\varepsilon^1)\\
&-\Omega_0 \frac{du^{(n)}}{ds} + f_u(0,0|u^{(n)}) = \sum_{i+j=n} \frac{n!}{i!\,j!}\{\Omega_1 \frac{du^{(j)}}{ds} - f_{u\omega}(0,0|u^{(i)})\omega_j +\\
&-\frac{1}{2!} f_{uu}(0,0|u^{(i)}|0^{(j)})\} - \sum_{i+j+k=n} \frac{n!}{i!\,j!\,k!} \ldots + \cdots (\varepsilon^n \quad \text{for} \quad n > 1).
\end{aligned}
\tag{13.63}
$$

Introducing the operator

$$
J_0(\cdot) \stackrel{\text{df}}{=} -\Omega_0 \frac{d(\cdot)}{ds} + f_u(0,0|(\cdot)), \tag{13.64}
$$

Equation (13.63) takes the following form

$$
\begin{cases}
J_0 u^{(1)} = 0,\\
J_0 u^{(n)} = g_n(s),
\end{cases}
\tag{13.65}
$$

where

$$
\begin{aligned}
&g_n(s) = g_n(s+2\pi) = n\Omega_{n-1} \frac{du^{(1)}}{ds} - n\omega_{n-1} f_{u\omega}(0,0|u^{(1)}) - R_{n-1},\\
&R_{n-1} = \sum_{i+j=n} \sum_{i,j\geq 1} \binom{n}{i} \frac{1}{2!} f_{uu}(0,0|u^{(i)}|u^{(j)}) + \sum_{i+j=n} \sum_{i\geq 2, j\geq 1} \frac{n!}{i!\,j!} \Big\{ -\Omega_j \frac{du^{(i)}}{ds}\\
&\quad + \omega_j f_{u\omega}(0,0|u^{(i)}) \Big\} + \sum_{i+j+k=n} \sum_{i,j,k\geq 1} \frac{n!}{i!\,j!\,k!} \Big\{ \frac{1}{2!} f_{u\omega\omega}(0,0|u^{(i)})\omega_j\omega_k\\
&\quad + \frac{1}{2!} f_{uu\omega}(0,0|u^{(i)}|u^{(j)})\omega_k + \frac{1}{3!} f_{uuu}(0,0|u^{(i)}|u^{(j)}|u^{(j)}) \Big\} + \cdots
\end{aligned}
\tag{13.66}
$$

Let us introduce the following harmonic functions

$$
z = qe^{is}, \quad z^* = q^* e^{is}. \tag{13.67}
$$

The following properties hold

$$
J_0 z = J_0 \bar{z} = 0, \tag{13.68}
$$

and

$$J_0^* \stackrel{\text{df}}{=} \Omega_0 \frac{d(\cdot)}{ds} + f_n(0,0|(\cdot)), \tag{13.69}$$

where: $f_u^* = A^*(0)u = A^T(0)u$.

The function z and $\bar{z}$ are linearly independent, and we assume the following orthogonality condition

$$[u, z^*] = \varepsilon. \tag{13.70}$$

This condition implies a chain of conditions

$$[u^{(1)}, z^*] = 1, \quad [u^{(n)}, z^*] = 0 \qquad for \quad n > 1. \tag{13.71}$$

In other words it means that the fundamental harmonic $e^{is}(e^{-is})$ appears only in $u^{(1)}$. The condition (13.70) gives an iteration for ε as the amplitude of the bifurcated solution. In order to solve (13.65), we assume

$$u^{(1)} = cz + \bar{c}\bar{z}, \tag{13.72}$$

where c is the complex constant.

The orthogonalization condition gives

$$[u^{(1)}, z^*] = c[z, z^*] = \bar{c}[z, z^*], \tag{13.73}$$

and hence $c = 1$ and

$$u^{(1)} = [z + z^*]. \tag{13.74}$$

The being sought periodic solution of (13.65) exists if the following orthogonality condition is satisfied (Fredholm alternative).

$$[g_n, z^*] = 0. \tag{13.75}$$

This condition eliminates the occurring secular terms from $g_n(s)$. Taking into account (13.72) and (13.74) in (13.75) we obtain the following complex equation

$$n\Omega_{n-1} i - n\omega_{n-1} < f_{u\omega}(0,0|q|q^*) > -[R_{n-1}, z^*] = 0 \tag{13.76}$$

with two unknowns Ω_{n-1} and ω_{n-1}. If $\sigma(\omega) = \xi(\omega) + i\eta(\omega)$ is the eigenvalue associated with the vector $q(\omega)$, then

$$\sigma q = f_u(\omega, 0|q). \tag{13.77}$$

Differentiating both sides of (13.75) with regard to ω and taking $\omega = 0$ we obtain

$$\{A(0) + i\,\Omega_0 I\}q_\omega(0) = \sigma_\omega(0) - f_{u\omega}(0, 0|q(0)), \tag{13.78}$$

where $q_\omega(0)$ is unknown. The Fredholm alternative applied to (13.78) gives

$$\langle \sigma_\omega(0)q(0) - f_{u\omega}(0, 0|q(0)), q^*\rangle = 0. \tag{13.79}$$

Taking into account the earlier introduced notation $q(0) = q$ and $q^*(0) = q^*$ ($\langle q, \bar{q}^*\rangle = 1$) we get

$$\sigma_\omega(0) =< f_{u\omega}(0, 0|q(0)), q^* > . \tag{13.80}$$

A solvability condition for $n > 1$ with regards to $u^{(n)} \in P_{2\pi}$ yields the equation

$$-n\Omega_{n-1}i + n\omega_{n-1}r_\omega(0) + [R_{n-1}, z^*] = 0. \tag{13.81}$$

Separating real and imaginary parts we obtain

$$\omega_{n-1} = -\frac{\mathrm{Re}[R_{n-1}, z^*]}{n\xi_\omega(0)} \tag{13.82}$$

and

$$\Omega_{n-1} = -\mathrm{Re}[R_{n-1}, z^*]\frac{\eta_{\omega(0)}}{\xi_\omega(0)} + \frac{1}{n}\mathrm{Im}[R_{n-1}, z^*]. \tag{13.83}$$

The obtained dependencies (13.82) and (13.83) allow to find the unknown coefficients. Taking $n = 2$, we get $R_1 = f_{uu}(0, 0|u^{(1)}|u^{(1)})$ and $[R_1, z^*] = 0$, which implies that $\omega_1 = \Omega_1 = 0$. It can be shown that

$$\omega_{2k-1} = \Omega_{2k-1} = 0 \qquad k \in \mathbb{N}. \tag{13.84}$$

It means that the functions $\omega(\varepsilon)$ i $\Omega(\varepsilon)$ are even.
In order to obtain ω_2 and Ω_2 we take $n = 3$, and we get

$$R_2 = \frac{3}{2}f_{uu}(0, 0|u^{(1)}|u^{(2)}) + f_{uuu}(0, 0|u^{(1)}|u^{(1)}|u^{(1)}). \tag{13.85}$$

To find $[R_2, z^*]$ one needs to solve (13.66) for $n = 2$ ($u^{(2)}(s)$). The right-hand side of $g_2(s)$ can be presented by

$$g_2 = -R_1 = -f_{uu}(0, 0|q|q)e^{i2s} - 2f_{uu}(0, 0|q|\bar{q}) - f_{uu}(0, 0|\bar{q}|\bar{q})e^{-i2s}, \tag{13.86}$$

where the condition $[g_2, z^*] = 0$ is always satisfied. Let us denote

$$-f_{uu}(0,0|q|q) = P, \; -2f_{uu}(0,0|q|q) = S, \tag{13.87}$$

and hence

$$g_2 = S + Pe^{i2s} + \bar{P}e^{-i2s} \tag{13.88}$$

The solution $u^{(2)}(s)$ of (13.65) is a sought in the form

$$u^{(2)}(s) = K + Le^{i2s} + \bar{L}e^{-i2s} \tag{13.89}$$

where K, L are real and complex vectors of the form

$$K = A^{-1}(0)S, L = \{A(0) - 2i\Omega_0 I\}^{-1}P, \tag{13.90}$$

where $A(0)$ and $A(0) - 2i\Omega_0 I$ are nonsingular.

Denoting

$$Le^{i2s} = y, \tag{13.91}$$

we obtain

$$f_{uu}(0,0|u^{(1)}|u^{(2)}) = f_{uu}(0,0|z+\bar{z}|K+y+\bar{y}) = f_{uu}(0,0|z|K) + f_{uu}(0,0|z|y) + f_{uu}(0,0|z|\bar{y}) + f_{uu}(0,0|\bar{z}|K) + f_{uu}(0,0|\bar{z}|y) + f_{uu}(0,0|\bar{z}|\bar{y}). \tag{13.92}$$

Applying orthogonalization to each term of (13.72) with z^* we obtain

$$[f_{uu}(0,0|u^{(1)}|u^{(2)}), z^*] = \langle (f_{uu}(0,0|q|K) + f_{uu}(0,0|q|L)), q^* \rangle = \sum_{i=1}^{n}\sum_{j=1}^{n}\sum_{k=1}^{n} b_{ijk}\bar{q_i^*}(q_j K_k + \bar{q_j} L_k), \tag{13.93}$$

where

$$b_{ijk} = \frac{\partial^2 f_i}{\partial u_j \partial u_k}|_{u=0,\omega=0}. \tag{13.94}$$

Noting that

$$[f_{uuu}(0,0|u^{(1)}|u^{(1)}|u^{(1)}), z^*] = 3\langle f_{uuu}(0,0|q|q|\bar{q}) \rangle = \sum_{i=1}^{n}\sum_{j=1}^{n}\sum_{k=1}^{n}\sum_{l=1}^{n} c_{ijkl}\bar{q_i^*} q_j q_k q_l, \tag{13.95}$$

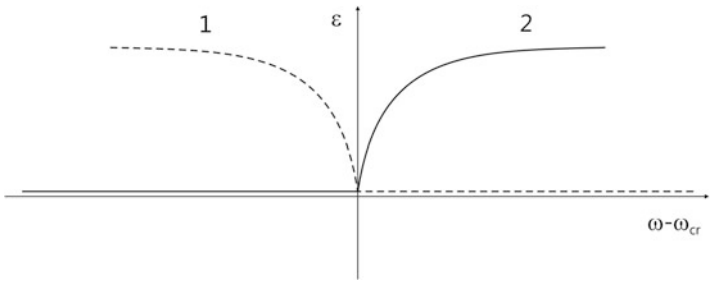

Fig. 13.14 Amplitude of the periodic solution versus the bifurcation parameter for sub-critical (*1*) and super-critical (*2*) bifurcation

where:

$$c_{ijkl} = \frac{\partial^3 f_i}{\partial u_j \partial u_k \partial u_l}|_{u=0,\omega=0}, \tag{13.96}$$

we obtain

$$\begin{aligned}[R_2, z^*] = \frac{3}{2}\langle f_{uu}(0,0|q|K) + f_{uu}(0,0|\bar{q}|L), q^*\rangle \\ +3\langle f_{uuu}(0,0|q|q|\bar{q}), q^*\rangle.\end{aligned} \tag{13.97}$$

The first-order approximation of the bifurcated solution is

$$u(s,\varepsilon) = \varepsilon u^{(1)}(s) = \varepsilon(z+\bar{z}) = 2\varepsilon \mathrm{Re}\{q^{is}\} = 2\varepsilon\{\mathrm{Re\ q}\cos\Omega(\varepsilon)t - \mathrm{Im\ q}\sin\Omega(\varepsilon)t\}, \tag{13.98}$$

where:

$$\Omega = \Omega_0 + \frac{1}{2}\varepsilon^2\Omega_2 \tag{13.99}$$

and

$$\omega = \omega_{cr} + \frac{1}{2}\varepsilon^2\omega_2. \tag{13.100}$$

The obtained dependence $\omega(\varepsilon)$ is shown in Fig. 13.14.

For $\omega_2 > 0$ a super-critical bifurcation occurs, whereas for $\omega_2 < 0$ a subcritical bifurcation appears. In the case of $\omega_2 = 0$ one has to calculate ω_4. Eliminating ε from (13.99) and (13.100) we obtain the dependence of self-excited frequency versus the bifurcation parameter

$$\Omega = \Omega_0 + \frac{\Omega_2}{\omega_2}(\omega - \omega_{cr}). \tag{13.101}$$

The second-order approximation to the bifurcated solution has the form

$$u(s,\varepsilon) = \varepsilon u^{(1)} + \frac{1}{2}\varepsilon^2 u^{(2)} = 2\varepsilon \mathrm{Re}\{q e^{is}\} + \frac{1}{2}\varepsilon^2 K + \varepsilon^2 \mathrm{Re}\{L e^{i2s}\}. \tag{13.102}$$

It is seen that it contains harmonic and superharmonic parts as well as the constant parts. The latter causes a shift of oscillation origin.

One can proceed in a similar way to get the successive approximations for $n = 3, 4, \ldots$.

For the first-order approximation we get

$$\begin{aligned}
\|u(s,\varepsilon)\| = \sqrt{[u,u]} &= \left\{ \frac{1}{2\pi} \int_0^{2\pi} < u, u > ds \right\}^{\frac{1}{2}} \\
&= \varepsilon \left\{ \frac{1}{2\pi} \int_0^{2\pi} \sum_{i=1}^{n} (q_i e^{is} + \bar{q}_i e^{-is})(\bar{q}_i e^{-is} + q_i e^{is}) ds \right\}^{\frac{1}{2}} \\
&= \varepsilon \left\{ \frac{1}{2\pi} \int_0^{2\pi} \sum_{i=1}^{n} (q_i^2 e^{i2s} + 2 q_i \bar{q}_i + (\bar{q}_i)^2 e^{-i2s}) ds \right\}^{\frac{1}{2}} \\
&= \varepsilon \left\{ 2 \sum_{i=1}^{n} 2 q_i \bar{q}_i \right\}^{\frac{1}{2}} = \varepsilon \left\{ 2 \sum_{i=1}^{n} |q_i|^2 \right\}^{\frac{1}{2}} = \varepsilon \sqrt{2} \|q\|.
\end{aligned} \tag{13.103}$$

In the second-order approximation we have

$$u(t,\omega) = 2\sqrt{\frac{2\omega}{\omega_2}} \mathrm{Re}\{q e^{i\Omega t}\} + \frac{\omega}{\omega_2} K + \frac{2\omega}{\omega_2} \mathrm{Re}\{L e^{i2\Omega t}\}. \tag{13.104}$$

The $\omega(\varepsilon)$ approximation using nth order polynomial

$$\omega(\varepsilon) = \omega_{cr} + \frac{1}{2}\omega_2 \varepsilon^2 + \frac{1}{24}\omega_4 \varepsilon^4 + O(\varepsilon^6) \tag{13.105}$$

yields the picture shown in Fig. 13.15.

The term ω_4 is defined by

$$\omega_4 = -\frac{\mathrm{Re}[R_4, z^*]}{5\xi_\omega(\omega_{cr})}, \tag{13.106}$$

where:

$$\begin{aligned}
R_4 = 30\omega_2 \langle f_{uu}(q|K) + f_{uu\omega}(\bar{q}|L) + f_{uuu\omega}(q|q|q), q^* \rangle \\
+15\langle f_{uuu}(q|K|K) + 2 f_{uuu}(\bar{q}|L|\bar{L}) + 2 f_{uuu}(\bar{q}|K|L), q^* \rangle.
\end{aligned} \tag{13.107}$$

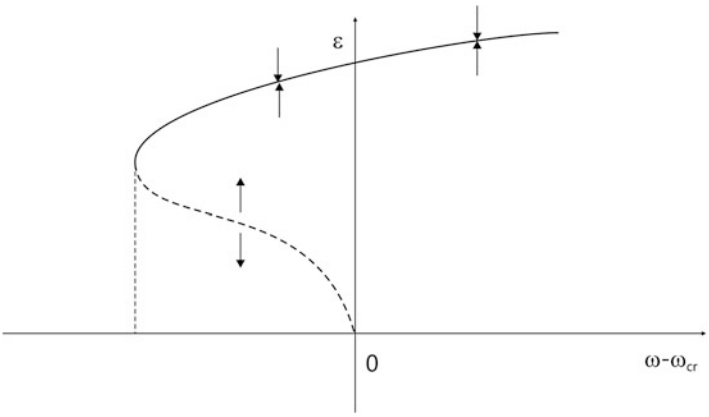

Fig. 13.15 Hopf bifurcation diagram

Now we briefly describe a stability estimation of the periodic bifurcated solution $V(s, \varepsilon)$ of Eq. (13.47). Considering v as the perturbation to the investigated solution V, i.e. by substituting

$$v = u - V \tag{13.108}$$

to (13.47) we get

$$\dot{v} = g(\omega, v, s, \varepsilon), \tag{13.109}$$

where

$$g(\omega, v, s, \varepsilon) = f(\omega, V + v) - f(\omega, V). \tag{13.110}$$

The linearized equation (13.109) has the form

$$\dot{v} = g_v(\omega, 0|v), \tag{13.111}$$

where

$$g_v(\omega, 0|v) = f_n(\omega, v(s, \varepsilon)|v). \tag{13.112}$$

Equation (13.111) has periodic coefficients. A stability of $v = 0$ depends on the eigenvalues of the monodromy matrix. One of the eigenvalues (Floquet exponents) is equal to zero, whereas the second depends analytically on ε, i.e. $\sigma = \sigma(\varepsilon)$ and $\sigma(0) = 0$.

Theorem 13.5 (Orbital Stability). *A limit cycle is asymptotical orbitally stable if all Floquet exponents have negative real parts.*

The next theorem gives hints how to find real Floquet exponents.

Theorem 13.6. *A real Floquet exponent $\sigma(\varepsilon)$ can be presented in the form*

$$\sigma(\varepsilon) = \hat{\sigma}(\varepsilon)\frac{d\omega}{d\varepsilon}, \tag{13.113}$$

where: $\hat{\sigma}(\varepsilon)$ is the smooth function in neighbourhood of $\varepsilon = 0$ such that $\frac{d\hat{\sigma}(\varepsilon)}{d\varepsilon}(0) = -\xi(0)$, and $\frac{\hat{\sigma}(\varepsilon)}{\varepsilon}$ is an even function. Since

$$\frac{d\omega}{d\varepsilon} = \varepsilon\omega_2 + O(\varepsilon^4) \tag{13.114}$$

and

$$\hat{\sigma}(\varepsilon) = -\xi_\omega(0)\varepsilon + O(\varepsilon^3), \tag{13.115}$$

therefore

$$\sigma(\varepsilon) = -\xi_\omega(0)\omega_2\varepsilon^2 + O(\varepsilon^4). \tag{13.116}$$

To conclude, we have two following cases:

(i) $\omega\xi_\omega(0) > 0$, and $\sigma(\varepsilon) < 0$. Then the solution is orbitally asymptotic stable;
(ii) $\omega\xi_\omega(0) < 0$, and $\sigma(\varepsilon) < 0$. Then the solution is orbitally unstable.

Example 13.4 (See [144]). We consider the Van der Pol equation of the following form

$$\begin{aligned} \dot{x_1} &= x_2, \\ \dot{x_2} &= -x_1 + \omega x_2 - x_1^2 x_2. \end{aligned}$$

The matrix of the linearized system in the vicinity of $(0, 0)$ is

$$A(\omega) = \begin{bmatrix} 0 & 1 \\ -1 & \omega \end{bmatrix}.$$

The eigenvalues of $A(\omega)$ are defined by the equation

$$\sigma^2 - \omega\sigma + 1 = 0.$$

Hence, for $|\omega| < 2$ there exist complex conjugate roots, whereas for $|\omega| \geq 2$ we have real eigenvalues $\sigma_2 << \sigma_1 < 0$ for $\omega < -2$, and $\sigma_1 > \sigma_2 > 0$ for $\omega > 2$. The complex conjugate roots are

$$\sigma_{1,2} = \frac{\omega}{2} \pm \frac{i}{2}\sqrt{4 - \omega^2}.$$

The trajectories of the eigenvalues σ_1 and σ_2 form the up and down half-circle of the complex plane $(\mathrm{Re}\,\sigma)^2 + (\mathrm{Im}\,\sigma)^2 = 1$. Depending on ω we have the following types of the singular points

(1) $\omega < -2$ (stable node);
(2) $\omega = -2$ (stable node degenerated);
(3) $-2 < \omega < 0$ (stable focus);
(4) $\omega = 0$ (asymptotically stable focus);
(5) $0 < \omega < 2$ (unstable focus);
(6) $\omega = 2$ (unstable node degenerated);
(7) $\omega > 2$ (unstable node).

Let us check the Hopf bifurcation theorem assumptions:

(i) $f(\omega, 0)$ for every $\omega, x = 0$ is isolated equilibrium;
(ii) the function f is analytical for $(x, \omega) \in \mathbb{R}^2 \times \mathbb{R}$;
(iii) the matrix $A(\omega)$ has a pair of complex eigenvalues such that $\mathrm{Re}\sigma_1(0) = \mathrm{Re}\sigma_2(0) = 0$, $\mathrm{Im}(\sigma_1) = 1 > 0$ and $\frac{d(\mathrm{Re}\sigma_1)}{d\omega}(0) = \frac{1}{2} \neq 0$.

The bifurcated solutions and the eigenvectors are defined by the equations that can be found using the Iooss and Joseph [127] method, and they are reported in [144]. □

13.2.5 Double Hopf Bifurcation

One may extend a concept of analysis of Hopf bifurcation into a case when a few pairs of purely imaginary eigenvalues cross an imaginary axis of the complex plane with nonzero velocities. Although there exist many papers devoted to this problem [73, 100, 164], but we follow here Dei Yu [250] research results.

If the Jacobian of higher-dimensional dynamical system possesses two pairs of purely imaginary eigenvalues, then the so-called double Hopf bifurcation may be exhibited. If the ratio of the two eigenvalues is not a rational number, then associated bifurcation in non-resonant.

Following Yu [250], consider the following dynamical system

$$\dot{\mathbf{x}} = Ax + F(x). \tag{13.117}$$

where: $x \in \mathbb{R}^n$, $F : \mathbb{R}^n \to \mathbb{R}^n$, $F(0) = F'(0) = 0$, and

$$A = \begin{bmatrix} 0 & \omega_{1c} & 0 & 0 & 0 \\ -\omega_{1c} & 0 & 0 & 0 & 0 \\ 0 & 0 & 0 & \omega_{2c} & 0 \\ 0 & 0 & -\omega_{2c} & 0 & 0 \\ 0 & 0 & 0 & 0 & B \end{bmatrix}. \tag{13.118}$$

Notice that B matrix is of order $(n-4)\times(n-4)$ and it is hyperbolic one, which means that its associated eigenvalues have no zero real parts. We assume also that $\omega_{1c}/\omega_{2c} \neq k/l$, where $k, l \in \mathbb{C}$.

In an explicit form Eq. (13.117) reads

$$\begin{aligned}
\dot{x}_1 &= \omega_{1c}x_2 + F_1(x), \quad \dot{x}_2 = -\omega_{1c}x_1 + F_2(x),\\
\dot{x}_3 &= \omega_{2c}x_4 + F_3(x), \quad \dot{x}_4 = -\omega_{2c}x_3 + F_4(x),\\
\dot{x}_p &= -\alpha_p x_p + F_p(x), \quad p = 5, 6, \ldots, m_1 + 4,\\
\dot{x}_q &= -\alpha_q x_q + \omega_q x_{q+1} + F_q(x), \quad \dot{x}_{q+1} = -\omega_q x_q - \alpha_q x_{q+1} + F_{q+1}(x),\\
&\qquad q = m_1 + 5, m_1 + 7, \ldots, n-1
\end{aligned} \tag{13.119}$$

and $n = 4 + m_1 + 2m_2$.

In what follows, the multiple time scale method is used assuming that $t = t(T_0, T_1, T_2, \ldots)$, and $T_0 = t$, $T_1 = \varepsilon t$, $T_2 = \varepsilon^2 t$, and so on. Therefore

$$\begin{aligned}
\frac{d}{dt} &= \frac{\partial}{\partial T_0}\frac{\partial T_0}{\partial t} + \frac{\partial}{\partial T_1}\frac{\partial T_1}{\partial t} + \frac{\partial}{\partial T_2}\frac{\partial T_2}{\partial t} + \cdots\\
&= D_0 + \varepsilon D_1 + \varepsilon^2 D_2 + \cdots .
\end{aligned} \tag{13.120}$$

A being sought solution is expanded into the power series with respect to ε

$$x_i(t;\varepsilon) = \varepsilon x_{i1}(T_0, T_1, T_2, \ldots) + \varepsilon^2 x_{i2}(T_0, T_1, T_2, \ldots) + \varepsilon^3 x_{i3}(T_0, T_1, T_2, \ldots) + \cdots \tag{13.121}$$

Substituting (13.121) into (13.2.5), and accounting (13.120) the following sequence of perturbation equations is obtained

$$\begin{aligned}
\varepsilon:\ & D_0 x_{11} = \omega_{1c}x_{21},\\
& D_0 x_{21} = -\omega_{1c}x_{11},\\
& D_0 x_{31} = \omega_{2c}x_{41},\\
& D_0 x_{41} = -\omega_{2c}x_{31},\\
& D_0 x_{p1} = -\alpha_p x_{p1},\\
& D_0 x_{q1} = -\alpha_q x_{q1} + \omega_q x_{(q+1)1},\\
& D_0 x_{(q+1)1} = -\omega_q x_{q1} + \alpha_q x_{(q+1)1};
\end{aligned} \tag{13.122}$$

$$\begin{aligned}
\varepsilon^2:\ & D_0 x_{12} = \omega_{1c}x_{22} - D_1 x_{11} + F_{12}(x_1),\\
& D_0 x_{22} = -\omega_{1c}x_{12} - D_1 x_{21} + F_{22}(x_1),\\
& D_0 x_{32} = \omega_{2c}x_{42} - D_1 x_{31} + F_{32}(x_1),\\
& D_0 x_{42} = -\omega_{2c}x_{32} - D_1 x_{41} + F_{42}(x_1),\\
& D_0 x_{p2} = -\alpha_p x_{p2} + F_{p2}(x_1),\\
& D_0 x_{q2} = -\alpha_q x_{q2} + \omega_q x_{(q+1)2} + F_{q2}(x_1),\\
& D_0 x_{(q+1)2} = -\omega_q x_{q2} + \alpha_q x_{(q+1)2} + F_{(q+1)2}x_1),
\end{aligned} \tag{13.123}$$

where x_1 corresponds to the first-order approximation and $f_{i2} = d^2[F_i(x)/\varepsilon]/d\varepsilon^2)_{\varepsilon=0}$ are the functions of x_1.

Differentiating the first of Eq. (13.122) and substituting the second equation into the resulting equation yields

$$D_0^2 x_{11} + \omega_{1c}^2 x_{12} = 0, \tag{13.124}$$

which has the following solution

$$x_{11} = r_1(T_1, T_2, \ldots) cos[\omega_{1c} T_0 + \Phi_1((T_1, T_2, \ldots)] \equiv r_1 cos\Theta_1, \tag{13.125}$$

where r_1 is the amplitude and Φ_1 is the phase. Knowing x_{11} it is easy to obtain x_{21} from the third equation of (13.122). Proceeding in a similar way one finds

$$x_{31} = r_2(T_1, T_2, \ldots) cos[\omega_{2c} T_0 + \Phi_2(T_1, T_2, \ldots)] \equiv r_2 cos\Theta_2, \tag{13.126}$$

and then x_{41} is defined by the fourth equation of (13.122). The other variables $x_{j1} = 0, \quad j = 5, 6, \ldots, n$.

Observe also that

$$D_0 r_1 = D_0 r_2 = 0, \qquad D_0\Phi_1 = D_0\Phi_2 = 0. \tag{13.127}$$

From Eq. (13.123) we obtain

$$D_0^2 x_{12} + \omega_{1c}^2 x_{12} = -D_1 D_0 x_{11} - \omega_{1c} D_1 x_{21} + D_0 F_{12} + \omega_{1c} F_{22}. \tag{13.128}$$

The condition for avoiding secular terms determine $D_1 r_i$ and $D_1\Phi_i, \quad i = 1, 2$. In the next step one finds the particular solution of (13.128). Having obtained x_{12} one easily finds x_{22} from the second equation of (13.123).

Using Eqs. (13.125) and (13.126) the following first-order differential equations are obtained

$$\frac{dr_i}{dt} = D_0 r_i + \varepsilon D_1 r_i + \varepsilon^2 D_2 r_i + \varepsilon^3 D_3 r_i + \cdots \tag{13.129}$$

$$\frac{d\Phi_i}{dt} = D_0\Phi_i + \varepsilon D_1\Phi_i + \varepsilon^2 D_2\Phi_i + \varepsilon^3 D_3\Phi_i + \cdots \tag{13.130}$$

Recall that we analyse non-resonant double Hopf bifurcation, and hence we get $D_{2k+1} r_i = D_{2k+1}\Theta_i = 0$ for $k = 0, 1, 2, \ldots$, whereas

$$\begin{aligned} D_{2k} r_1 &= r_1[a_{2k0} r_1^{2k} + a_{(2k-2)2} r_1^{2k-1} r_2^2 + \cdots + a_{2(2k-2)} r_1^{2k-1} + a_{02k} r_2^{2k}], \\ D_{2k} r_2 &= r_2[b_{2k0} r_1^{2k} + b_{(2k-2)2} r_1^{2k-1} r_2^2 + \cdots + b_{2(2k-2)} r_1^2 r_2^{2k-2} + b_{02k} r_2^{2k}] \end{aligned} \tag{13.131}$$

and $D_{2k}\Phi_i$ have similar form.

Introducing a back scaling $\varepsilon x_i \to x_i, \quad \varepsilon r_i \to r_i$, Eqs. (13.129), (13.130) have the new form

$$\frac{dr_i}{dt} = D_2 r_i + D_4 r_i + D_6 r_i + \cdots \tag{13.132}$$

$$\frac{d\Phi_i}{dt} = D_2 \Phi_i + D_4 \Phi_i + D_6 \Phi_i + \cdots \tag{13.133}$$

and

$$\frac{d\Theta_i}{dt} = \omega_{ic} + \frac{d\Phi_i}{dt}, \tag{13.134}$$

where: $\Theta_i = \omega_{ic} T_0 + \Phi_i \equiv \omega_{ic} t + \Phi_i$, and $i = 1, 2, \ldots$.

It is worth noticing that Eqs. (13.132), 13.133) and (13.134) are called *normal forms*. A reason is that $D_{2k} r_1$, $D_{2k} r_2$, $D_{2k} \Phi_1$ and $D_{2k} \Phi_2$ are obtained by eliminating *secular* terms (i.e. resonant terms). The *resonant* terms are actually applied in Poincaré normal form theory.

Furthermore, the obtained periodic solution given by (13.124)–(13.126) and (13.132)–(13.134) represents both asymptotic and transient solution for the *critical* variables (modes) $x_i, \quad i = 1, 2, 3, 4 \quad (r_i = r_i(t)$, and $\Phi_i = \Phi_i(t))$. The *non-critical* variables (modes) $x_j, \quad j = 5, 6, \ldots$ are found from Eq. (13.121) (they are excited by critical variables),

Observe also that the periodic solution (13.121) can be treated as the nonlinear transformation between (13.117) and the normal forms (13.132)–(13.134). This observation is supported by the following consideration. The periodic solution can be written as

$$\begin{aligned}
x_1 &= r_1 \cos\Theta_1 + h_1(r_1 \cos\Theta_1, r_1 \sin\Theta_1, r_2 \cos\Theta_2, r_2 \sin\Theta_2), \\
x_2 &= -r_1 \sin\Theta_1 + h_2(r_1 \cos\Theta_1, r_1 \sin\Theta_1, r_2 \cos\Theta_2, r_2 \sin\Theta_2), \\
x_3 &= r_2 \cos\Theta_2 + h_3(r_1 \cos\Theta_1, r_1 \sin\Theta_1, r_2 \cos\Theta_2, r_2 \sin\Theta_2), \\
x_4 &= -r_2 \sin\Theta_2 + h_4(r_1 \cos\Theta_1, r_1 \sin\Theta_1, r_2 \cos\Theta_2, r_2 \sin\Theta_2), \\
x_i &= h_i(r_1 \cos\Theta_1, r_1 \sin\Theta_1, r_2 \cos\Theta_2, r_2 \sin\Theta_2), \quad i = 5, 6, \ldots, n.
\end{aligned} \tag{13.135}$$

Introducing the new variables

$$y_1 = r_1 \cos\Theta_1, \quad y_2 = -r_2 \sin\Theta_1, \quad y_3 = r_2 \cos\Theta_2, \quad y_4 = -r_2 \sin\Theta_2, \tag{13.136}$$

from (13.135) one gets

$$x_i = y_i + h_i(y_1, y_2, y_3, y_4), \quad i = 1, 2, 3, 4, \quad x_i = h_j(y_1, y_2, y_3, y_4), \quad i = 5, 6, \ldots, n. \tag{13.137}$$

The obtained equation, which is the same as (13.121), manifests a transformation between $x_i, \quad i = 1, 2, \ldots, n$ and $y_j, \quad j = 1, 2, 3, 4$. In other words, the first four equations can be considered as a nonlinear transformations between the coordinates x_1, x_2, x_3, x_4 and y_1, y_2, y_3, y_4. The remaining equations represent the projection of the original system to the four-dimensional centre manifold governed by the critical variables y_1, y_2, y_3, y_4. Using the Cartesian coordinates the normal form governed by (13.132)–(13.134) reads

$$\begin{aligned}
\dot{y}_1 &= \omega_{1c} y_2 + g_1(y_1, y_2, y_3, y_4), \\
\dot{y}_2 &= -\omega_{1c} y_1 + g_2(y_1, y_2, y_3, y_4), \\
\dot{y}_3 &= \omega_{2c} y_4 + g_3(y_1, y_2, y_3, y_4), \\
\dot{y}_4 &= -\omega_{2c} y_3 + g_4(y_1, y_2, y_3, y_4).
\end{aligned} \tag{13.138}$$

To sum up, the nonlinear transformation (13.138), which is equivalent to (13.121), represents a transition between the original system (13.117) and the normal form (13.138).

Now both stability and bifurcation analysis may be carried out using Eqs. (13.132)–(13.134) or (13.138).

Following Yu [250], in order to outline a general bifurcational analysis, the normal form is presented explicitly up to third order

$$\dot{r}_1 = r_1[\alpha_{11}\mu_1 + \alpha_{12}\mu_2 + a_{20}r_1^2 + a_{02}r_2^2], \dot{r}_2 = r_2[\alpha_{21}\mu_1 + \alpha_{22}\mu_2 + b_{20}r_1^2 + b_{02}r_2^2], \tag{13.139}$$

and similarly

$$\dot{\Theta}_1 = \omega_{1c} + \beta_{11}\mu_1 + \beta_{12}\mu_2 + c_{20}r_1^2 + c_{02}r_2^2, \dot{\Theta}_2 = \omega_{2c} + \beta_{21}\mu_1 + \beta_{22}\mu_2 + d_{20}r_1^2 + d_{02}r_2^2, \tag{13.140}$$

For the convenience two parameter variables $\alpha_{11}\mu_1 + \alpha_{12}\mu_2, \quad \alpha_{21}\mu_1 + \alpha_{22}\mu_2$ are used, where μ_1, μ_2 are the perturbation parameters.

The tracked behaviour follows:

1. Equilibria (E):

$$r_1 = r_2 = 0 \tag{13.141}$$

2. Hopf bifurcation with frequency ω_1 ($H(\omega_1)$):

$$r_1^2 = -\frac{1}{a_{20}}(\alpha_{11}\mu_1 + \alpha_{12}\mu_2), r_2 = 0, \omega_1 = \omega_{1c} + \beta_{11}\mu_1 + \beta_{12}\mu_2 + c_{20}r_1^2. \tag{13.142}$$

3. Hopf bifurcation with frequency ω_2 ($H(\omega_2)$):

$$r_2^2 = -\frac{1}{b_{02}}(\alpha_{21}\mu_1 + \alpha_{22}\mu_2), r_1 = 0, \omega_2 = \omega_{2c} + \beta_{21}\mu_1 + \beta_{22}\mu_2 + d_{02}r_2^2. \tag{13.143}$$

4. 2-D tori with frequencies ω_1, ω_2 (2-D tori):

$$
\begin{aligned}
r_1^2 &= -\frac{a_{02}(\alpha_{21}\mu_1 + \alpha_{22}\mu_2) - b_{02}(\alpha_{11}\mu_1 + \alpha_{12}\mu_2)}{a_{20}b_{02} - a_{02}b_{20}}, \\
r_2^2 &= -\frac{b_{20}(\alpha_{21}\mu_1 + \alpha_{12}\mu_2) - a_{20}(\alpha_{21}\mu_1 + \alpha_{22}\mu_2)}{a_{20}b_{02} - a_{02}b_{20}}, \\
\omega_1 &= \omega_{1c} + \beta_{11}\mu_1 + \beta_{12}\mu_2 + c_{20}r_1^2 + c_{02}r_2^2, \\
\omega_2 &= \omega_{2c} + \beta_{21}\mu_1 + \beta_{22}\mu_2 + d_{20}r_1^2 + d_{02}r_2^2.
\end{aligned} \tag{13.144}
$$

Evaluating the Jacobian of Eq. (13.139) on the equilibrium (13.141) yields two critical lines

$$L_1: \qquad \alpha_{11}\mu_1 + \alpha_{12}\mu_2 = 0 \quad (\alpha_{21}\mu_1 + \alpha_{22}\mu_2 < 0), \tag{13.145}$$

$$L_2: \qquad \alpha_{21}u_1 + \alpha_{22}u_2 = 0 \quad (\alpha_{11}u_1 + \alpha_{12}u_2 < 0), \tag{13.146}$$

and L_1 (L_2) corresponds to occurrence of a family of periodic solutions after Hopf bifurcation with ω_1 (ω_2). The solutions are stable if the following inequalities are satisfied

$$\alpha_{11}\mu_1 + \alpha_{12}\mu_2 > 0 \quad \text{and} \quad \alpha_{21}\mu_1 + \alpha_{22}\mu_2 < 0. \tag{13.147}$$

Now, evaluating the Jacobian of Eq. (13.139) on the Hopf bifurcation solution (13.142), yields the stability conditions

$$\alpha_{11}\mu_1 + \alpha_{22}\mu_2 > 0 \quad \text{and} \quad \alpha_{21}\mu_1 + \alpha_{22}\mu_2 - \frac{b_{20}}{a_{20}}(\alpha_{11}\mu_1 + \alpha_{12}\mu_2) < 0. \tag{13.148}$$

One may check that the $H(\omega_1)$ periodic solution exists, when $a_{20} < 0$.

The second inequality in (13.148) yields the critical line

$$L_3: \quad (\alpha_{21} - \frac{b_{20}}{a_{20}}\alpha_{11})\mu_1 + (\alpha_{22} - \frac{b_{20}}{a_{20}}\alpha_{12})\mu_2 = 0 \quad (\alpha_{11}\mu_1 + \alpha_{12}\mu_2) > 0). \tag{13.149}$$

The L_3 line represents a secondary Hopf bifurcation with frequency ω_2 from the limit cycle produced by $H(\omega_1)$ (i.e. a 2-D torus is created).

Similarly, the (13.143) solution associated with $H(\omega_2)$ is stable when the inequalities hold

$$\alpha_{21}\mu_1 + \alpha_{22}\mu_2 > 0 \quad \text{and} \quad \alpha_{11}\mu_1 + \alpha_{12}\mu_2 - \frac{a_{02}}{b_{02}}(\alpha_{21}\mu_1 + \alpha_{22}\mu_2) < 0 \tag{13.150}$$

and it exists when $b_{02} < 0$.

A critical line L_4 is defined by the second inequality of (13.150):

$$L_4: \quad (\alpha_{11} - \frac{a_{02}}{b_{02}}\alpha_{21})\mu_1 + (\alpha_{12} - \frac{a_{02}}{b_{02}}\alpha_{22})\mu_2 = 0 \quad (\alpha_{11}\mu_1 + \alpha_{22}\mu_2) > 0). \tag{13.151}$$

Crossing L_4 a secondary Hopf bifurcation with frequency ω_1 occurs from the periodic orbits born after $H(\omega_2)$. Again the 2-D tori is produced, with solutions, governed by Eq. (13.144).

In [250] a family of solutions lying on 2-D tori is traced via evaluation the Jacobian on Eq. (13.144) yielding

$$\mathbf{J_T} = \begin{bmatrix} 2a_{20}r_1^2 & 2a_{02}r_1r_2 \\ 2b_{20}r_1r_2 & 2a_{02}r_2^2 \end{bmatrix}. \tag{13.152}$$

The stability of the quasi-periodic motion is defined by trace (Tr $<$ 0) and determinant (Det $>$ 0) of the Jacobian $\mathbf{J_T}$.

The mentioned stability conditions are supplemented by the following existence conditions

$$\begin{aligned} &a_{02}(\alpha_{21}\mu_1 + \alpha_{22}\mu_2) - b_{02}(\alpha_{21}\mu_1 + \alpha_{12}\mu_2) > 0, \\ &b_{20}(\alpha_{11}\mu_1 + \alpha_{12}\mu_2) - a_{20}(\alpha_{21}\mu_1 + \alpha_{22}\mu_2) > 0. \end{aligned} \tag{13.153}$$

Observe that the existence region boundaries (13.153) are defined by the critical lines L_3 and L_4, i.e. the periodic solution associated with $H(\omega_1)$ ($H(\omega_2)$) bifurcates from the critical line L_3 (L_4) into a quasi-periodic solution with the stability boundary L_3 (L_4).

Note that $r_1 > 0$ and $r_2 > 0$ guarantee satisfaction of conditions (13.153), and $Det > 0$ yields

$$a_{20}b_{02} - a_{02}b_{20} > 0, \tag{13.154}$$

and hence the condition $Tr < 0$ gives

$$a_{20}(a_{02} - b_{02})(\alpha_{21}\mu_1 + \alpha_{22}\mu_2) - b_{02}(a_{22} - b_{20})(\alpha_{11}\mu_1 + \alpha_{12}\mu_2) < 0. \tag{13.155}$$

From (13.155) one gets

$$\begin{aligned} &L_5: [a_{20}(a_{02} - b_{02})\alpha_{21} - b_{02}(a_{22} - b_{20})\alpha_{11}]\mu_1 \\ &+[a_{20}(a_{02} - b_{02})\alpha_{22} - b_{02}(a_{22} - b_{20})\alpha_{12}]\mu_2 = 0. \end{aligned} \tag{13.156}$$

On L_5 a quasi periodic solution may loose its stability, and bifurcate to a 3-D torus with frequencies $(\omega_1, \omega_2, \omega_3)$.

A combination of perturbation approaches and harmonic balance technique to analyse various Hopf type bifurcations is presented in works [18–21, 30] and examples of numerical technique to trace dynamical behaviour using a path following method taken from mechanics and biomechanics are reported in [15–17].

13.3 Fixed Points of Maps

There are three distinct situations possible for bifurcations of fixed points of maps.

(i) $D_x f(x_0, \lambda_0)$ *has a single eigenvalue equal to 1.*

In this case the problem is reduced to a study of one-dimensional centre manifold

$$x \mapsto f(x, \lambda), \quad x \in \mathbb{R}^1, \ \lambda \in \mathbb{R}^1. \tag{13.157}$$

Fixed point can be transformed to the origin, where $f(0,0) = 0$ and $\frac{\partial f}{\partial x}(0,0) = 1$. In this case three situations are possible.

A *saddle-node bifurcation* at $(x, \lambda) = (0,0)$ takes place if

$$\begin{aligned} &f(0,0) = 0, \\ &\tfrac{\partial f}{\partial \lambda}(0,0) = 1, \end{aligned} \tag{13.158}$$

and

$$\begin{aligned} &\frac{\partial f}{\partial \lambda}(0,0) \neq 0, \\ &\frac{\partial^2 f}{\partial x^2}(0,0) \neq 0. \end{aligned} \tag{13.159}$$

The map

$$x \mapsto f(x, \lambda) = x + \lambda \pm x^2, \quad x \in \mathbb{R}^1, \quad \lambda \in \mathbb{R}^1 \tag{13.160}$$

can serve as a normal form for the saddle-node bifurcations for maps.

A *transcritical bifurcation* can be represented by the map

$$x \mapsto f(x, \lambda) = x + \lambda x \pm x^2, \quad x \in \mathbb{R}^1, \quad \lambda \in \mathbb{R}^1. \tag{13.161}$$

Note that $(x, \lambda) = (0,0)$ is a non-hyperbolic fixed point with eigenvalue 1 ($f(0,0) = 0$, $\frac{\partial f}{\partial x}(0,0) = 1$). A transcritical bifurcation appears if

$$\frac{\partial f}{\partial \lambda}(0,0) = 0, \quad \frac{\partial^2 f}{\partial x \partial \lambda}(0,0) \neq 0, \quad \frac{\partial^2 f}{\partial x^2}(0,0) \neq 0. \tag{13.162}$$

A *pitchfork bifurcation* occurs in a one parameter family of smooth one-dimensional maps (13.157) with a non-hyperbolic fixed point ($f(0,0) = 0$, $\frac{\partial f}{\partial x}(0,0) = 1$) if

$$\frac{\partial f}{\partial \lambda}(0,0)=0,\quad \frac{\partial^2 f}{\partial x^2}(0,0)=0,\quad \frac{\partial^2 f}{\partial x\partial \lambda}(0,0)\neq 0,\quad \frac{\partial^3 f}{\partial x^3}(0,0)\neq 0, \tag{13.163}$$

and its normal form is given by

$$x\mapsto f(x,\lambda)=x+\lambda x\pm x^3,\quad x\in\mathbb{R}^1,\quad \lambda\in\mathbb{R}^1. \tag{13.164}$$

(ii) $D_x f(x_0,\lambda_0)$ *has a single eigenvalue equal to* -1.
In contrary to the bifurcation (i) this bifurcation does not have an analog with one-dimensional dynamics of vector fields, since it refers to period-doubling bifurcation at $(x,\lambda)=(0,0)$. It occurs when

$$\begin{aligned} &f(0,0)=0,\quad \frac{\partial f}{\partial x}(0,0)=-1,\quad \frac{\partial f}{\partial \lambda}(0,0)=0,\\ &\frac{\partial^2 f}{\partial x^2}(0,0)=0,\quad \frac{\partial^2 f}{\partial x\partial \lambda}(0,0)\neq 0,\quad \frac{\partial^3 f}{\partial x^3}(0,0)\neq 0. \end{aligned} \tag{13.165}$$

One can display the period-doubling bifurcation using the map

$$x\mapsto f(x,\lambda)=-x-\lambda x+x^3. \tag{13.166}$$

(iii) $D_x f(x_0,\lambda_0)$ *possesses two complex conjugate eigenvalues having modulus 1.*
This situation corresponds to the Neimark–Sacker bifurcation or sometimes it is referred as a secondary Hopf bifurcation ([106, 243]).

Consider the map (13.157) but for $x\in\mathbb{R}^2$, and let us again introduce a suitable transformation that $(x,\lambda)=(0,0)$ and $f(0,0)$. The associated matrix $D_x f(0,0)$ possesses two complex conjugate eigenvalues $\lambda(0)$ and $\bar{\lambda}(0)$, with $|\lambda(0)|=1$. In addition, we require that $\lambda^n(0)\neq 1$ for $n=1,2,3,4$.

It can be shown [243] that the normal form of the Neimark–Sacker bifurcation is governed by the complex map

$$z\mapsto \mu(\lambda)z+c(\lambda)z^2\bar{z}+O(4),\quad z\in\mathbb{C},\ \lambda\in\mathbb{R}^1. \tag{13.167}$$

We change the variables letting

$$z=re^{2\pi i\Theta}, \tag{13.168}$$

and we get

$$\begin{aligned} &r\mapsto |\mu(\lambda)|\left(r+\left(\mathrm{Re}\left(\frac{c(\lambda)}{\mu(\lambda)}\right)\right)r^3+O(r^4)\right),\\ &\Theta\mapsto \Theta+\phi(\lambda)+\frac{1}{2\pi}\left(\mathrm{Im}\left(\frac{c(\lambda)}{\mu(\lambda)}\right)\right)r^2+O(r^3), \end{aligned} \tag{13.169}$$

where

$$\phi(\lambda) \equiv \frac{1}{2\pi}\tan^{-1}\frac{\omega(\lambda)}{\alpha(\lambda)},$$
$$c(\lambda) = \alpha(\lambda) + i\omega(\lambda). \tag{13.170}$$

The Taylor expansion of (13.169) in $\lambda = 0$ gives

$$r \mapsto \left(1 + \frac{d}{d\lambda}|\mu(\lambda)|\,|_{\lambda=0}\lambda\right) r + \left(\mathrm{Re}\left(\frac{c(0)}{\mu(0)}\right)\right) r^3 + O(\lambda^2 r, \lambda r^3, r^4),$$
$$\Theta \mapsto \Theta + \phi(0) + \frac{d}{d\lambda}\phi(\lambda)|_{\lambda=0}\lambda + \frac{1}{2\pi}\left(\mathrm{Im}\frac{c(0)}{\mu(0)}\right) r^2. \tag{13.171}$$

The truncated normal form has the form

$$r \mapsto r + (d\lambda + ar^2)r,$$
$$\Theta \mapsto \Theta + \phi_0 + \phi_1\lambda + br^2, \tag{13.172}$$

where

$$d = \frac{d}{d\lambda}|\mu(\lambda)|_{\lambda=0},\ a = \mathrm{Re}\left(\frac{c(0)}{\mu(0)}\right),\ \phi_0 = \phi(0),\ \phi_1 = \frac{d}{dx}(\phi(\lambda)),\ b = \frac{1}{2\pi}\mathrm{Im}\frac{c(0)}{\lambda(0)}. \tag{13.173}$$

Following [243] there are four potential cases for the bifurcation of an invariant circle from a fixed point.

(a) $d > 0$, $a > 0$. The origin is an unstable fixed point for $\lambda > 0$ and an asymptotically stable fixed point for $\lambda < 0$ with an unstable invariant circle for $\lambda < 0$.
(b) $d > 0$, $a < 0$. The origin is an unstable fixed point for $\lambda > 0$ and an asymptotically stable fixed point for $\lambda < 0$ with an asymptotically stable invariant circle for $\lambda > 0$.
(c) $d > 0$, $a < 0$. The origin is an asymptotically stable fixed point for $\lambda > 0$ and an unstable fixed point for$\lambda < 0$ with an unstable invariant circle for $\lambda > 0$.
(d) The origin is an asymptotically stable fixed point for $\lambda > 0$, and an unstable fixed point for $\lambda < 0$, with an asymptotically stable invariant circle for $\lambda < 0$.

Note that here the bifurcation consists of a circle which has many different orbits. Hence one should start with the initial condition laying on this circle. Since in this case $r = (-\frac{\lambda d}{a})^{\frac{1}{2}}$, then the associated circle map has the form

$$\Theta \mapsto \Theta + \phi_0 + \left(\phi_1 + \frac{d}{a}\right)\lambda. \tag{13.174}$$

For $\phi_0 + (\phi_1 + \frac{d}{a})\lambda$ rational (irrational) all orbits on invariant circle are periodic (quasiperiodic, i.e. densely fill the circle).

13.4 Continuation Technique

The introduced earlier considerations related to local bifurcations can be used to follow the dynamics in a systematic way. In a case of vector fields, one can construct a local Poincaré map, and then to reduce the problem of one order to study a bifurcation of a fixed point of the map. In a case of a k periodic orbit one can take into account the bifurcation of a fixed point of the kth iterate of the map.

Coming back to the differential equation (13.1) and taking into account the initial condition $x(t_0) = x_0$ (for a given specific numerical value of λ_0) one can trace a periodic orbit occurred via Hopf bifurcation. We integrate numerically (13.1) during the time equal to exact (or estimated) period of a new periodic orbit corresponding to the parameter $\lambda_0 + \Delta\lambda$, where $\|\Delta\lambda\| \ll 1$.

In a case of second-order differential equation the situation is shown in Fig. 13.16.

In a case of periodic solution with the period T_0 we have the following boundary condition

$$x(T_0, x_0) - x_0 = 0. \tag{13.175}$$

Equation (13.175) yields x_0 using, for instance, Newton's method. Using Taylor expansion around kth order approximation of $x_0^{(k)}$ we take only a linear term, and we obtain a linear correction $\Delta x_0^{(k)}$. A Jacobian of the Newton method is defined by

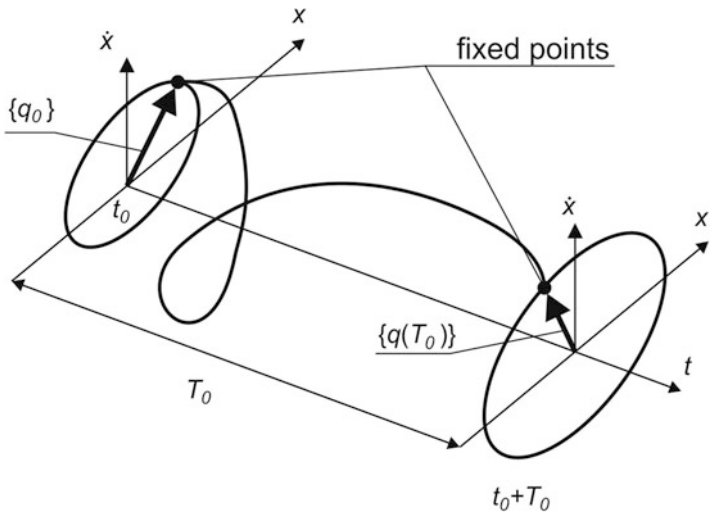

Fig. 13.16 Transformation of the state vector x_0

$$J = \frac{\partial x(T_0, x_0)}{\partial x_0} - I = N - I, \tag{13.176}$$

where I is the identity matrix. After computation with the required accuracy we use the matrix N obtained in the last computational step as the monodromy matrix. The associated eigenvalues decide about stability and bifurcation of the analysed periodic orbit (or equivalently, a fixed point of the maps). This method is called shooting and has already found a wide treatment in literature (see, for instance Seydel [214], Awrejcewicz [14]).

Another equivalent approach is based on the Galerkin approximation [234]. It is well known that any periodic solution (function) can be represented by its Fourier expansion

$$y_k = a_0 + \sum_{k=1}^{K} (a_{c_k} \cos k\omega t + a_{s_k} \sin k\omega t), \tag{13.177}$$

where K is the number of a highest harmonics, and ω is the fundamental frequency. The assumed solution is substituted to the system of the second-order differential equations governing dynamics of oscillating systems. Since from the assumption we have the kth order Fourier approximation to a periodic solution, then between left- and right-hand sides a difference occurs (a residual vector), which satisfies the equation

$$r(a_0, a_{c_k}, a_{s_k}, t) = r(a_0, a_{c_k}, a_{s_k}, t + T). \tag{13.178}$$

In general, when $K \to \infty$, then $r \to 0$. The residual vector is also expanded into Fourier series

$$r = s_0 + \sum_{k=1}^{K} (s_{c_k} \cos k\omega t + s_{s_k} \sin k\omega t). \tag{13.179}$$

The condition $r = 0$ implies that $s_0 = s_{c_k} = s_{s_k} = 0$, and hence

$$\begin{aligned}
&\frac{1}{T} \int_0^T r(a_0, a_{c_k}, a_{s_k}, t) dt = 0, \\
&\frac{2}{T} \int_0^T r(a_0, a_{c_k}, a_{s_k}, t) \cos n\omega t dt = 0, \\
&\frac{2}{T} \int_0^T r(a_0, a_{c_k}, a_{s_k}, t) \sin n\omega t dt = 0, \quad k, n = 1, 2, 3, \ldots
\end{aligned} \tag{13.180}$$

Introducing the vectors

$$s = \begin{pmatrix} s_0 \\ s_{c_k} \\ s_{s_k} \end{pmatrix}, \quad a = \begin{pmatrix} a_0 \\ a_{c_k} \\ a_{s_k} \end{pmatrix}, \tag{13.181}$$

equation $r = 0$ can be substituted by

$$s(a) = 0, \tag{13.182}$$

and can be solved using the iterational Newton method. In practice the Fast Fourier Transformation (FFT) is used during computation of s [49,71]. After an appropriate choice of a starting point for the vector **a** we compute

$$\begin{aligned} \dot{y_k} &= \sum_{k=1}^{K} (k\omega a_{s_k} \cos k\omega t - k\omega a_{c_k} \sin k\omega t), \\ \ddot{y_k} &= \sum_{k=1}^{K} (-k^2\omega^2 a_{c_k} \cos k\omega t - k^2\omega^2 a_{s_k} \sin k\omega t). \end{aligned} \tag{13.183}$$

Applying $(\text{FFT})^{-1}$ we can find (13.183), then we substitute (13.183) into the governing equations to get (13.182). The FFT is especially economic when a number of samples N_{FFT} satisfies $N_{\text{FFT}} = 2^M > 4K$. The error of the introduced estimation is equal to

$$\Delta = \left(\sum_{n=k+1}^{\frac{N_{\text{FFT}}}{2}} (s_{c_{n_k}}^2 + s_{s_{n_k}}^2) \right)^{\frac{1}{2}}. \tag{13.184}$$

A stability of the found solution is estimated by the variational equations.

Example 13.5. Consider a model of human vocal chords oscillations (see more details in [15–17]). The human lungs produces the air pressure required for larynx to be opened. The vocal chords start to continue to open because of inertia, and then their elastic properties cause their closing. The air stream leaves the larynx, and then Bernoulli suction effect appears. Next the described cycle repeats. Display a bifurcation diagram corresponding to the mechanical model of human vocal chords shown in Fig. 13.17.

A point mass can move in the directions x and y. Since the vocal chords cannot touch each other, the artificial damping c_s and stiffness k_s have been introduced. The hyperbolic type stiffness associated with the coefficient k_s approaches infinity when the mass approaches origin. The larynx has been modelled as a reservoir with stiff walls and real elastic properties have been included in the modified air

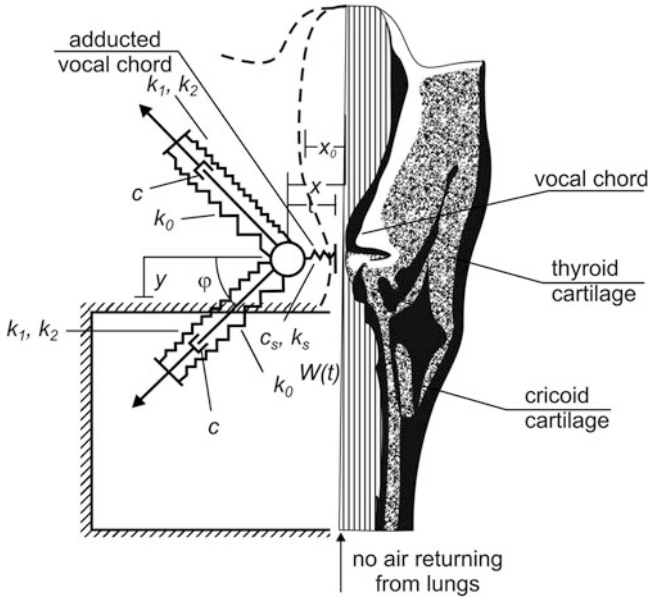

Fig. 13.17 Mechanical model of a human vocal chord

parameters. It is assumed that the lungs pressure generates equal forces acting on the vocal chords, which move symmetrically. This is a reason that we consider only one vocal chord oscillations. In a case of some pathological cases (for instance caused by cancer) the symmetry is violated and the number of equations is doubled.

The ordinary non-dimensional differential equations have the form (see [17] for more details)

$$\ddot{X} + C\dot{X} + \{K_x + K_D[(X - X_0)^2 + Y^2]\}(X - X_0) - K_{xy}Y -$$
$$-K_s X^{-s}(1 - C_s\dot{X}) = EP,$$
$$\ddot{Y} + C\dot{Y} + \{K_y + K_D[(X - X_0)^2 + Y^2]\}Y - K_{xy}(X - X_0) = EP,$$
$$\dot{P} = Q - \begin{cases} (X-1)P^{0,5}, \text{ for } X > 1, \\ 0, \text{ for } x \leq 1. \end{cases}$$

where: C corresponds to damping properties of the vocal chords ($C < 1$); K_y represents a vertical stiffness of a vocal chord ($K_y \in (0,7; 0,9)$), $K_x = 1$; K_{xy} is the stiffness coefficient coupling the vocal chord displacements in two directions $K_{xy} \in (0,3; 0,5)$); K_0 is a Duffing (cubic) type stiffness coefficient ($K_0 < 1$); K_s is a coefficient of a hyperbolic type stiffness ($K_s < 0,1$); $s = 4$; C_s represents damping ($C_s < 1$); X_0 is the horizontal equilibrium position of the vocal chord; E is the average surface of the vocal chord ($E \in (0,1; 0,0)$) and Q is outlay of the air stream ($Q \in (0,0; 100,0)$).

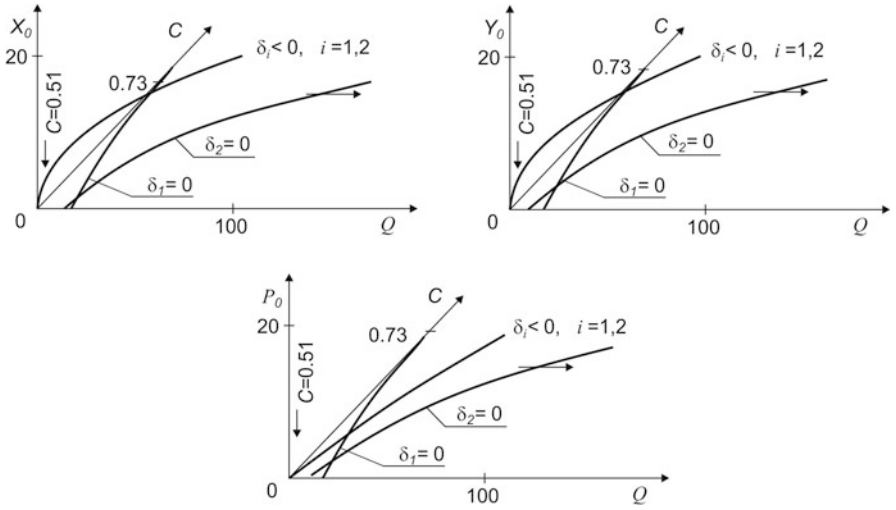

Fig. 13.18 Equilibrium and stability

The analysed system of differential equations is strongly nonlinear especially in a vicinity of origin (see the term responsible for hyperbolic type stiffness). We take the following fixed parameters: $K_y = O.9; K_{xy} = 0.3; K_0 = 0.001; K_s = 0,001; C_s = 0.5; E = 1$. First we calculate equilibria positions (see Fig. 13.18).

The solid curves in the planes (X_0, Q), (Y_0, Q) and (P_0, Q) correspond to the equilibrium positions. They do not change with the change of C, but their stability depends on C. The solid curves located in the plane (C, Q) correspond to stability loss boundaries.

Denote the eigenvalues associated with an equilibrium by $\lambda_{1,2} = \delta_1 \pm i\omega_1, \lambda_{3,4} = \delta_2 \pm i\omega_2$ (it can be proved that the fifth eigenvalue is real and negative). If $\delta_i = 0$ $(i = 1, 2)$, then for a fixed C value the Hopf bifurcation occurs with an increase or decrease of Q (see directions of vertical arrows). A point of intersection of both curves can be interpreted as a meeting point of two frequencies ω_1 and ω_2. If they are irrational then a quasi-periodic orbit appears.

The bifurcation diagram for $K_y = 0.3$; $K_D = K_s = 0.001$; $D_s = 0.5$; $K_{xy} = 0.3$; $X_0 = E = 0.4$; $Q = 7$ has been reported in Fig. 13.19, and the calculations have been carried out using shooting method.

Damping coefficient C has been taken as an active parameter. Its decrease causes occurrence of the Hopf bifurcation and a periodic orbit appears (this is example of self-exciting oscillations). A slight further decrease of C yields an increase of the oscillation amplitude represented by the branch $1'$. In the point $PD1'$ we have period doubling bifurcation and a new subharmonic solution appears (branch $3'$). This solution is further traced numerically along this branch and in the point Q it changes its stability. As the numerical analysis shown in the vicinity of Q a quasi-periodic solution appears.

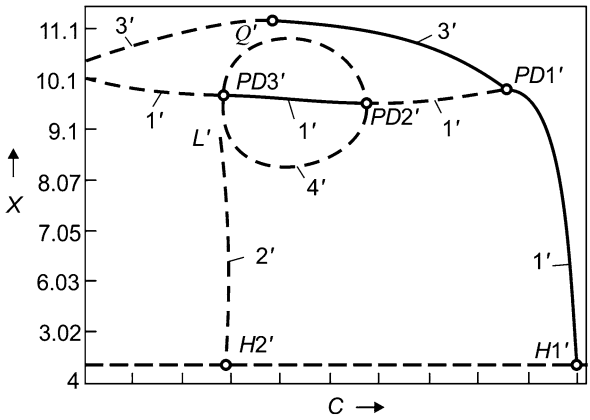

Fig. 13.19 Bifurcation diagram of the human vocal chords

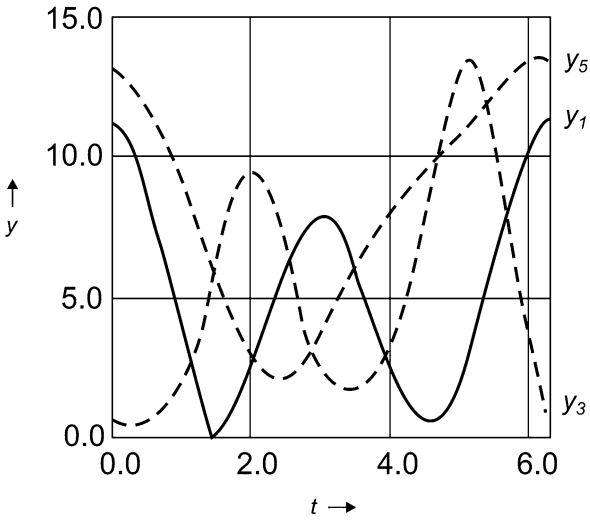

Fig. 13.20 Periodic oscillation for vocal chords

The branch 1 becomes unstable in the point $PD1'$. However between $PD2'$ and $PD3$ we have stable periodic solution. In the point $H2'$ another periodic solution branch appears which is unstable.

It is clear that for each point of the bifurcation curve one can easily obtain phase trajectories or time histories. For instance, the latter are shown in Fig. 13.20 for $C = 0.16$.

During calculations the period has been normalized to 2π and (from this figure) it is seen that this a subharmonic stable solution of the branch $3'$. A cusp of y_i is visible, which is in agreement with our hyperbolic type stiffness assumption. It must be emphasized that in this case the shooting method is much more economical in comparison to the Urabe–Reiter method. In the latter case one needs to take high number of harmonics which extremely extends computation time. The shooting method does not have the mentioned drawback. □

13.5 Global Bifurcations

As it has been pointed out in monographs [216,217], sometimes a periodic orbit does not exist on the stability boundary and Poincaré map is not defined i.e. it cannot be analysed using a local approach.

First we can consider *bifurcation of a homoclinic loop to a saddle-node equilibrium*, which is displayed by the equations

$$\begin{aligned} \dot{x_1} &= \mu + \lambda_2 x^2 + G(x_1, \mu), \\ \dot{x_2} &= [A + h(x_1, x_2, \mu)]x_2, \end{aligned} \tag{13.185}$$

where the eigenvalues of A lie in LHP (see Fig. 13.21).

For $\mu < 0$ saddle O_1 and a node O_2 are distinct. They approach each other when $\mu \to 0^+$. In the critical point $\mu = 0$ the saddle-node equilibrium with the homoclinic loop disappears and a stable periodic orbit P_μ is born with a period of $\pi/\sqrt{\mu\lambda_2}$. In fact this observation can be formulated as a theorem and proved (see [216]).

We give one more example taken from [85], where two mutually coupled oscillators are considered:

$$\begin{aligned} \dot{x}_1 &= x_2, \\ \dot{x}_2 &= -\varepsilon(1 - \beta {x_1}^2 + {x_1}^4)x_2 - x_1 + \alpha x_3, \\ \dot{x}_3 &= x_4, \\ \dot{x}_4 &= -\varepsilon(1 - \beta {x_3}^2 + {x_3}^4)x_4 - x_3 + \alpha x_1, \end{aligned} \tag{13.186}$$

where $0 < \alpha < 1$ is a coupling factor, β controls amplitude and ε is a control parameter. It has been shown that two symmetric solutions disappear simultaneously for $\varepsilon = 0.448$ via saddle-node bifurcation. Just before this value a switching between two symmetric solutions occurred. The situation is displayed in Fig. 13.22.

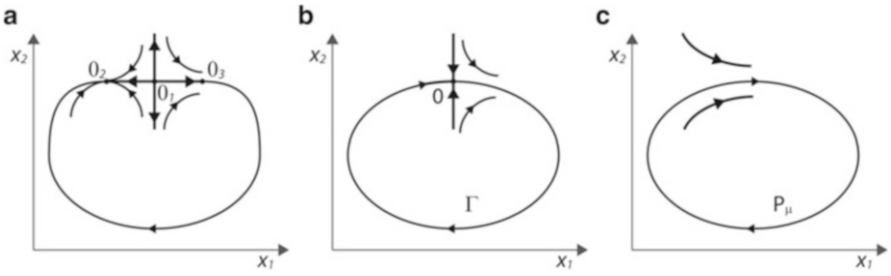

Fig. 13.21 Successive steps of a bifurcation of a saddle-node equilibrium with a homoclinic trajectory

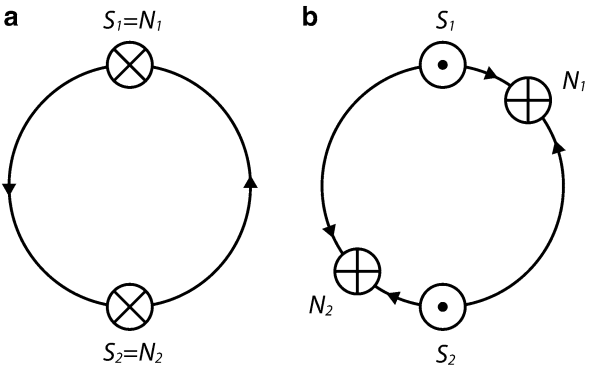

Fig. 13.22 A heteroclinic cycle at (**a**) and after (**b**) saddle-node bifurcation

The authors using Poincaré map, traced the unstable manifold W_n of the saddle in a vicinity of the saddle-node bifurcation and they observed the following scenario (see Fig. 13.22). One W_n of S_1 goes in N_1, whereas the other W_n goes in N_2. One of W_n of S_2 goes in N_1 and the other W_n of it goes in N_2. A node and a saddle coalesce at the saddle-node bifurcation point creating a degenerate saddle. A heteroclinic cycle links two degenerate saddles at this point. Two stable N_1 and N_2 are connected by unstable manifolds even after disappearance of the synchronized solution via saddle-node bifurcation and nodes are replaced by their traces. A flow stays traced of N_1 and N_2 for a relatively long time and then quickly moves along a heteroclinic cycle linking two traces.

Another important global bifurcation can lead to occurrence of an *invariant torus* or *Klein bottle*, which has been analysed by Afraimovich and Shilnikov ([1, 2]).

Theorem 13.7 (See [216]). *If the global unstable set of the saddle-node is a smooth compact manifold (a torus or a Klein bottle) at $\mu = 0$, then a smooth closed attractive invariant manifold T_μ (a torus or a Klein bottle, respectively) exists for all small μ.*

With a continuous change of μ, the invariant manifold will change continuously. For $\mu < 0$ we have a set composed of the unstable manifold of the saddle periodic orbit $P^-(\mu)$ with the stable periodic orbit $P^+(\mu)$ (by $P^\pm(\mu)$ we denote periodic orbits occurred after the saddle-node bifurcations). The invariant manifold for $\mu = 0$ is represented by w^u_p. For $\mu > 0$ the Poincaré rotation number approaches zero for $\mu \to 0^+$ (in case of torus). Hence, on the axis μ there are infinitely many phase-locking (resonant) zones (periodic orbits) as well as infinitely many zones composed of irrational values of μ (quasiperiodic orbits).

More detailed analysis of the briefly mentioned global bifurcations is given in the monograph [216] and is beyond of this book. There are also many references which include examples of various bifurcations in mechanics (see, for example [38, 145, 153, 190, 212, 231]).

Finally the basic phenomena of bifurcations exhibited by continuous dynamical systems, as well as explicit procedures for application of mathematical theorems to particular real-world problems are widely reported in monograph [146].

13.6 Piece-Wise Smooth Dynamical System

13.6.1 Introduction

The piece-wise smooth dynamical systems (PSDS) are governed by the equation:

$$\dot{x} = F(x;\lambda), \tag{13.187}$$

where: $x = x(t) \in \mathbb{R}^n$ represents the system state in time instant t; $\lambda \in \mathbb{R}^m$ is the vector of parameters, whereas the transformation $F : \mathbb{R}^n \times \mathbb{R}^m \to \mathbb{R}^n$ is the piece-wise smooth function. In other words, the phase space $D \in \mathbb{R}^n$ is divided into finite number of subspaces V_i, where the function F is smooth. The subspaces are separated by $(n-1)$ hyperplanes Σ_{ij}, where the 'discontinuities' are exhibited.

The PSDS governed by (13.187) can be classified in the following manner:

(i) Systems with discontinuous Jacobian DF, with continuous but non-smooth vector field F, and with smooth system's state $x(t)$;
(ii) Systems with discontinuous vector field F and with non-smooth but continuous $x(t)$;
(iii) Systems with discontinuous $x(t)$. In this case, whenever the system is in contact with Σ_{ij}, its state undergoes a jump described by $x^+ = g(x^-;\lambda)$, where $x^-(x^+)$ describes the system state just before (after) a contact.

Dynamical systems belonging to class (i) are often called Filippov systems [93,152]. In mechanical and electrical engineering there exist many various systems with piece-wise linear characteristics (see for example [46, 47, 161, 256]). Non-smooth mechanical systems with impact and/or friction have very long history and are described in many books (see, for instance [29] and references therein). Systems with Coulomb friction can be treated as those with a jump of a damping characteristics (class (ii))—see [95,151,152], or they exhibit a stick-slip movement. A stick takes place, when a resulting force acting on a moving body is less than the associated Coulomb force. Often the authors use differential inclusions in order to attack this problem more rigorously (see [143]). Three simple examples of mechanical systems with piece-wise nonlinearities are shown in Fig. 13.23.

In the first case (Fig. 13.23a) the system is governed by the equation

$$m\ddot{x} + F(x) = 0, \tag{13.188}$$

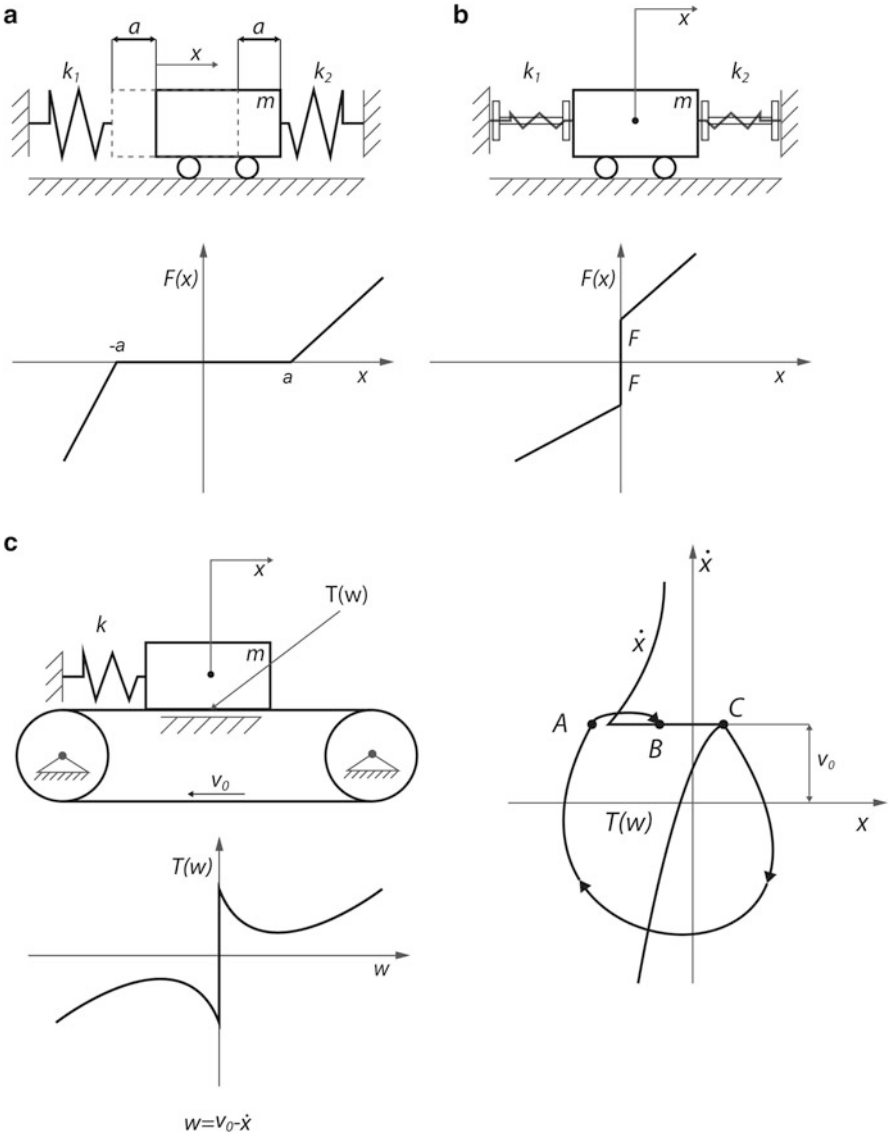

Fig. 13.23 One-degree-of-freedom system with a gap (**a**), discontinuous force (**b**), and stick-slip periodic motion (**c**)

where

$$F(x) = \begin{cases} 0 & \text{for } -a \le x \le a, \\ k_2(x-a) & \text{for } x > a, \\ k_1(x+a) & \text{for } x < a. \end{cases} \tag{13.189}$$

In the points $\pm a$ the function $F(x)$ is not differentiable. In the second case (Fig. 13.23b) the springs are initially stretched and governing differential equation is the same as (13.188), but

$$F(x) = \begin{cases} k_2 x + F_0 & \text{for } x > 0, \\ 0 & \text{for } x = 0, \\ k_1 x - F_0 & \text{for } x < 0. \end{cases} \tag{13.190}$$

In the third case the system is self-exited and is governed by equation

$$m\ddot{x} + kx = T(w) - T(0), \tag{13.191}$$

where:

$$T(w) = mg[\mu_0 \cdot sgnw - \alpha w + \beta w^3], \quad \omega = v_0 - \dot{x}. \tag{13.192}$$

In the above μ_0, α, β are coefficients describing friction. Note that the periodic orbit is not differentiable in the points A, B, C and the interval BC corresponds to stick, i.e. the mass m does not move in relation to tape. The system shown in Fig. 13.23a belongs to class (i), the system presented in Fig. 13.23b belongs to class (ii), and system given in Fig. 13.23c belongs to class (iii). The mechanical systems with impacts can be either modelled as a system with the sudden stiffness change (class (ii)), or as systems belonging to class (iii). In the latter case, when a surface $\Sigma_{i,j}$ is achieved, a sudden change of velocity occurs owing to the Newton's law and a definition of the restitution coefficient. In this case the system can be considered as that of one sided constraints and its behaviour is governed by algebraic inequalities. The described situation is equivalent also to a Dirac impulse of the function F on one of two sides of hyperplane $\Sigma_{i,j}$.

It is clear that in mechanical systems various classes of discontinuities may appear simultaneously. Although often friction and impact are independent ([238]) but more realistic are situations, where impact and friction appear together.

13.6.2 Stability

Here we consider a simple situation when on $\Sigma_{i,j}$ discontinuities do not occur. Recall also that when an analysed orbit belongs to any subspace V_i, than situation is clear, since stability concepts of smooth systems can be applied. Therefore, a stability devoted to PSDS is more general and when $\Sigma_{i,j}$ vanishes it is reduced to classical (smooth) stability concepts.

Assume that a periodic orbit $x(t)$ of a PSDS intersects the hyperplanes $\Sigma_{i,j}$ finite times in a periodic manner, and the intersections are non-degenerated, i.e. an orbit intersects $\Sigma_{i,j}$ transversally, a contact time with $\Sigma_{i,j}$ is infinitely short and all $\Sigma_{i,j}$ are smooth in contact points.

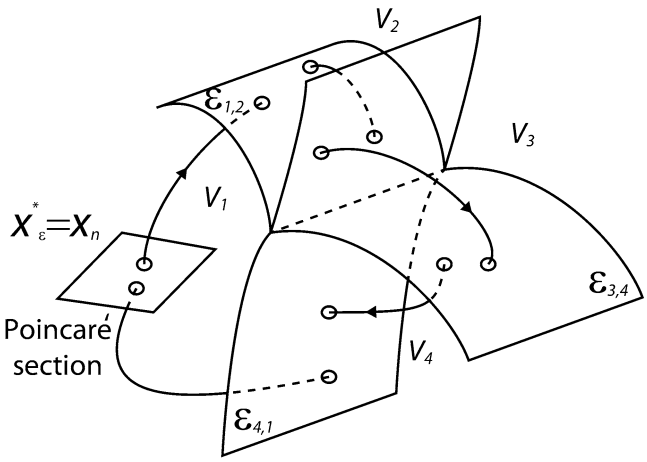

Fig. 13.24 A piece-wise smooth periodic orbit and a Poincaré section Σ

One may introduce a Poincaré section Σ which do not overlap with any $\Sigma_{i,j}$. In what follows we are going to analyse locally an intersection point of x(t) with Σ (further referred as x^*_Σ). To estimate stability one has to define a monodromy matrix ϕ^* owing to our earlier considerations for completely smooth systems. In order to obtain ϕ^* corresponding to piece-wise smooth periodic orbit, consider the matrix of fundamental solutions $\phi(t, t_0)$ satisfying the following linear differential equations

$$\dot{\phi}(t, t_0) = DF_i(x(t))\phi(t, t_0), \quad \phi(t, t_0) = I, \tag{13.193}$$

where D is the differential operator and DF_i denotes Jacobian. Observe that in time intervals $D_i = \{t \in \mathbb{R}; t_{i-1} < t < t_i\}$, for $i = 1, 2, \ldots, k+1$, the orbit $x(t)$ belongs to subspace V_i, where $F = F_i$ is smooth, and $F_{k+1} = F_1$ (see also Fig. 13.24 for $k = 4$). In each of the intersection (discontinuous) points defined by $t = t_i$ the orbit undergoes sudden changes, which means that the fundamental matrix also changes in these points. These changes can be formally expressed in the following way

$$\phi(t_i^+, t_0) = S_i \phi(t_i^-, t_0), \qquad i = 1, 2, \ldots, k. \tag{13.194}$$

In the above the superscript (−) denotes time instant just before a discontinuity, whereas the superscript (+) denotes time instant just after a discontinuity, and S_i is called saltation matrix.

In order to obtain explicitly a saltation matrix, one has to trace perturbations of two neighbourhood orbits $x(t)$ and $\overline{x}(t)$ (see Fig. 13.25).

The described method has been introduced for class (ii) by Aizerman–Gantmakher [3], and has been extended to the systems with discontinuous vector state [175].

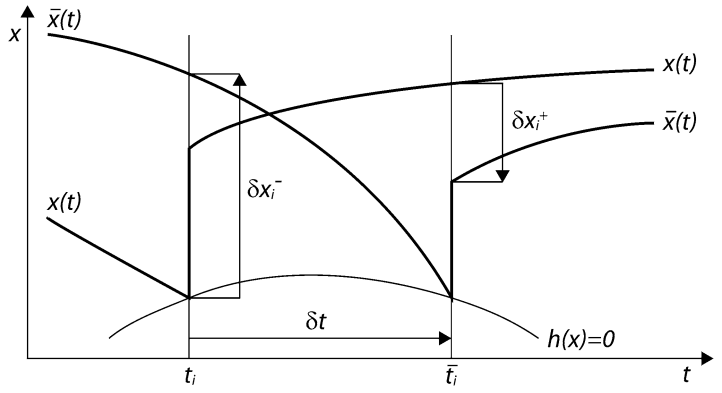

Fig. 13.25 Perturbed $\bar{x}(t)$ and unperturbed $x(t)$ orbits and the associated perturbations

Let us trace the orbit $x(t)$ in the time intervals D_i and D_{i+1}:

$$\begin{aligned} \dot{x} &= F_i(x), && \text{for } t_{i-1} < t < t_i, \\ 0 &= h_i(x_i^-), && \text{for } t = t_i, \\ x_i^+ &= g_i(x_i^-), && \text{for } t = t_i, \\ \dot{x} &= F_{i+1}(x), && \text{for } t_i < t < t_{i+1}, \end{aligned} \tag{13.195}$$

where: $x_i^- = \lim\limits_{\substack{t \to t_i \\ t<t_i}} x(t)$, $x_i^+ = \lim\limits_{\substack{t \to t_i \\ t>t_i}} x(t)$. Note that in the time instant $t = t_i$ defined by zero of smooth function $h_i(x)$ in V_i a discontinuity appears and in general the system state can exhibit a jump defined by a smooth function $g_i(x)$. In addition, it can happen that $F_i \neq F_{i+1}$. The function $h_i(x)$ can be scalar (for example during impacts in mechanical systems), or it can be a vector.

The perturbed solution $\bar{x}(t) = x(t) + \delta x(t)$ touches the constraint in time instant

$$\bar{t}_i = t_i + \delta t_i, \tag{13.196}$$

and it satisfies Eq. (13.195), where now the bars over x have to be added.

Assuming $\delta t_i > 0$ and following the introduced notations shown in Fig. 13.25, one obtains

$$\delta x_i^- = \bar{x}(t_i) - x_i^-, \delta x_i^+ = \bar{x}_i^+ - x(\bar{t}_i). \tag{13.197}$$

Since the perturbed orbit $\bar{x}(t)$ for $t = \bar{t}_i$ satisfies (13.195), the Taylor series expansions is used and the following manipulations hold:

$$\begin{aligned} 0 = h_i(\bar{x}_i^-) &= h_i\left(\bar{x}(t_i + \delta t_i)\right) \\ &\approx h_i(\bar{x}(t_i) + \frac{d\bar{x}}{dt} \mid_{t_i} \delta t_i) \end{aligned}$$

$$
\begin{aligned}
&\approx h_i(\bar{x}(t_i) + F_i(\bar{x}(t_i))\delta t_i) \\
&\approx h_i(x_i^- + \delta x_i^- + F_i(x_i^- + \delta x_i^-)\delta t_i) \\
&\approx h_i(x_i^- + \delta x_i^- + F_i(x_i^-)\delta t_i + DF_i(x_i^-)\delta x_i^- \delta t_i) \\
&\approx h_i(x_i^- + \delta x_i^- + F_i(x_i^-)\delta t_i) \\
&\approx h_i(x_i^-) + Dh_i(x_i^-)\delta x_i^- + Dh_i(x_i^-)F_i(x_i^-)\delta t_i. \qquad (13.198)
\end{aligned}
$$

Finally, the following equation is obtained

$$
Dh_i(x_i^-)[\delta x_i^- + F_i(x_i^-)\delta t_i] = 0. \qquad (13.199)
$$

In order to realize a non-degenerated contact between the orbit and discontinuous hyperplane $\Sigma_{i,j}$ the following condition should be assumed

$$
\text{rank}\, Dh_i(x_i^-)F_i(x_i^-) = \text{rank}[Dh_i(x_i^-)F_i(x_i^-), Dh_i(x_i^-)\delta x_i^-]. \qquad (13.200)
$$

From (13.199) one obtains

$$
\delta t_i = -\frac{Dh_i(x_i^-)\delta x_i^-}{Dh_i(x_i^-)F_i(x_i^-)}. \qquad (13.201)
$$

Now the Taylor series is applied to Eq. (13.195) and the manipulations similar to those in (13.198) are carried out:

$$
\begin{aligned}
\overline{x}_i^+ = g_i(\bar{x}_i^-) &\approx g_i(x_i^- + \delta x_i^- + F_i(x_i^-)\delta t_i) \\
&\approx g_i(x_i^-) + Dg_i(x_i^-)[\delta x_i^- + F_i(x_i^-)\delta t_i] \\
&\approx x_i^+ + Dg_i(x_i^-)[\delta x_i^- + F_i(x_i^-)\delta t_i]. \qquad (13.202)
\end{aligned}
$$

From (13.195), (13.197) and (13.202) one gets

$$
\begin{aligned}
\delta x_i^+ &= \overline{x}_i^+ - x(\bar{t}_i) \\
&\approx x_i^+ + Dg_i(x_i^-)[\delta x_i^- + F_i(x_i^-)\delta t_i] - (x_i^+ - \delta x_i^+) \\
&\approx x_i^+ + Dg_i(x_i^-)[\delta x_i^- + F_i(x_i^-)\delta t_i] - (x_i^+ + \dot{x}_i^+ \delta t_i) \\
&\approx x_i^+ + Dg_i(x_i^-)[\delta x_i^- + F_i(x_i^-)\delta t_i] - (x_i^+ + F_{i+1}(x_i^+)\delta t_i), \qquad (13.203)
\end{aligned}
$$

which finally yields

$$
\delta x_i^+ = Dg_i(x_i^-)\delta x_i^- + [Dg_i(x_i^-)F_i(x_i^-) - F_{i+1}(x_i^+)]\delta t_i, \qquad (13.204)
$$

and δt_i is defined by (13.201). Recall that the saltation matrix transforms the perturbation δx_i^- just before a discontinuity point into the perturbation δx_i^+ just after the discontinuity point via formula

$$\delta x_i^+ = S_i \delta x_i^-. \tag{13.205}$$

Hence, accounting (13.204) and (13.201), the saltation matrix is found

$$S_i = Dg_i(x_i^-) + [F_{i+1}(x_i^+) - Dg_i(x_i^-)F_i(x_i^-)]\frac{Dh_i(x_i^-)}{Dh_i(x_i^-)F_i(x_i^-)}. \tag{13.206}$$

Note that similar considerations can be repeated for $\delta t_i < 0$.

The introduced theory can be used as an extension of earlier one to trace through the described continuation technique the piece wise smooth periodic orbits and also classical algorithms for computations of Lyapunov exponents in smooth systems [89, 244, 245] (one has to include jumps of $\delta x(t)$ in each of discontinuity points) can be applied.

Example 13.6. Derive a saltation matrix using the Aizerman–Gantmakher theory in one-degree-of-freedom mechanical system with an impact.

The following second-order differential equation governs dynamics with impacts of the oscillator

$$\ddot{q} = F_q(q, \dot{q}, t), \qquad q \le q_{\max},$$

where $q_{\max}$ defines a barrier position. Assume that in the time instant $t = t_k, q(t_k) = q_{\max}$ and an impact modelled within Newton's hypothesis

$$\dot{q}^+ = -e\dot{q}^-$$

occurs, where: $\dot{q}^- = \dot{q}^-(t_k) = \lim\limits_{\substack{t \to t_k \\ t < t_k}} \dot{q}(t)$ is the oscillator velocity just before impact, whereas $\dot{q}^+ = \dot{q}^+(t_k) = \lim\limits_{\substack{t \to t_k \\ t > t_k}} \dot{q}(t)$ is the oscillator velocity just after impact, and e is the restitution coefficient. The following phase coordinates are introduced

$$x = \mathrm{col}\{x_1, x_2, x_3\} = \mathrm{col}\{q, \dot{q}, t\}.$$

Hence, we have

$$\dot{x} = F(x), \qquad x \in \mathbb{R}^3,$$

where

$$F(x) = \mathrm{col}\{x_2, F_q(x), 1\} = \mathrm{col}\{\dot{q}, F_q, 1\}.$$

The phase space configuration is defined by the inequality

$$h(x) \geq 0,$$

where $h(x) = q_{\max} - x_1 = q_{\max} - q$.

In the time instant $t = t_k$ defined by $h(x^-(t_k)) = 0$, we get

$$x^+ = g(x^-),$$

where: $x^- = x^-(t_k) = \lim\limits_{\substack{t \to t_k \\ t < t_k}} x(t)$, $x^+ = x^+(t_k) = \lim\limits_{\substack{t \to t_k \\ t > t_k}} x(t)$. The function defining a jump of the state vector in the point of discontinuity has the form

$$g(x) = \mathrm{col}\{x_1, -ex_2, x_3\} = \mathrm{col}\{q, -e\dot{q}, t\}.$$

The associated Jacobians with $h(x)$ and $g(x)$ have the form

$$Dh(x) = \begin{bmatrix} -1 & 0 & 0 \end{bmatrix},$$

$$Dg(x) = \begin{bmatrix} 1 & 0 & 0 \\ 0 & -e & 0 \\ 0 & 0 & 1 \end{bmatrix}.$$

From (13.201) one gets

$$\delta t = -\frac{Dh(x^-)\delta x^-}{Dh(x^-)F(x^-)} = -\frac{\begin{bmatrix} -1 & 0 & 0 \end{bmatrix} \begin{Bmatrix} \delta x_1^- \\ \delta x_2^- \\ \delta x_3^- \end{Bmatrix}}{\begin{bmatrix} -1 & 0 & 0 \end{bmatrix} \begin{Bmatrix} x_2^- \\ F_q^- \\ 1 \end{Bmatrix}} = -\frac{\delta x_1^-}{x_2^-} = -\frac{\delta q^-}{\dot{q}^-},$$

where $F_q^- = F_q(x^-)$.

Observe that for a degenerated impact, when $\dot{q}^- \to 0$, the time δt approaches infinity. The saltation matrix is obtained from (13.206):

$$S = Dg(x^-) + [F(x^+) - Dg(x^-)F(x^-)]\frac{Dh(x^-)}{Dh(x^-)F(x^-)}$$

$$
\begin{aligned}
&= \begin{bmatrix} 1 & 0 & 0 \\ 0 & -e & 0 \\ 0 & 0 & 1 \end{bmatrix} + \left(\begin{Bmatrix} \dot{q}^+ \\ F_q^+ \\ 1 \end{Bmatrix} - \begin{bmatrix} 1 & 0 & 0 \\ 0 & -e & 0 \\ 0 & 0 & 1 \end{bmatrix} \begin{Bmatrix} \dot{q}^- \\ F_q^- \\ 1 \end{Bmatrix} \right) \frac{\begin{bmatrix} -1 & 0 & 0 \end{bmatrix}}{\begin{bmatrix} -1 & 0 & 0 \end{bmatrix} \begin{Bmatrix} \dot{q}^- \\ F_q^- \\ 1 \end{Bmatrix}} \\
&= \begin{bmatrix} 1 & 0 & 0 \\ 0 & -e & 0 \\ 0 & 0 & 1 \end{bmatrix} + \left(\begin{Bmatrix} \dot{q}^+ \\ F_q^+ \\ 1 \end{Bmatrix} - \begin{Bmatrix} \dot{q}^- \\ -eF_q^- \\ 1 \end{Bmatrix} \right) \frac{\begin{bmatrix} -1 & 0 & 0 \end{bmatrix}}{(-\dot{q}^-)} \\
&= \begin{bmatrix} 1 & 0 & 0 \\ 0 & -e & 0 \\ 0 & 0 & 1 \end{bmatrix} + \begin{bmatrix} -(\dot{q}^+ - \dot{q}^-) & 0 & 0 \\ -(F_q^+ + eF_q^-) & 0 & 0 \\ 0 & & 0 \; 0 \end{bmatrix} (-\dot{q}^-)^{-1} \\
&= \begin{bmatrix} \dot{q}^+/\dot{q}^- & 0 & 0 \\ (F_q^+ + eF_q^-)/\dot{q}^- & -e & 0 \\ 0 & 0 & 1 \end{bmatrix},
\end{aligned}
$$

where $F_q^+ = F_q(x^+)$, and it can be cast to the following form

$$
S = \begin{bmatrix} -e & 0 & 0 \\ (F_q^+ + eF_q^-)/\dot{q}^- & -e & 0 \\ 0 & 0 & 1 \end{bmatrix}.
$$

The obtained matrix transforms a perturbation δx^- just before a barrier into the perturbation just after the barrier δx^+. It is worth noticing that in the case of grazing bifurcation (tangent to the barrier surface), the velocity $\dot{q}^- \to 0$, and possesses matrix element $S_{21} \to \infty$.

13.6.3 Orbits Exhibiting Degenerated Contact with Discontinuity Surfaces

In the previous section the eigenvalues of Jacobian changed smoothly with a smooth change of a bifurcation parameter. Hence, the analysed piecewise smooth orbits can exhibit all bifurcations described earlier and associated with smooth systems.

Here, we are going to analyse the cases, where a Poincaré map (or a vector field during analysis of stationary points), its Jacobian and the associated eigenvalues exhibit discontinuities, which are associated with smooth changes of a bifurcation parameter. In this case either the obtained bifurcations are qualitatively similar to those in smooth systems, or they are completely new.

The most explored bifurcation in PSDS is a so-called grazing bifurcation. It occurs, when a part of trajectory becomes tangent to one of the discontinuity surfaces while changing a bifurcation parameter smoothly. It cannot be predicted by

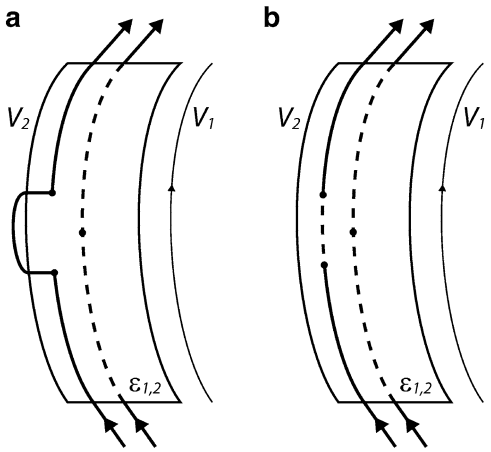

Fig. 13.26 Grazing bifurcations exhibited by Filippov's system (**a**) and a system with discontinuous vector state (**b**)

tracing a Jacobian behaviour. This type of bifurcation has been extensively studied by Feigin ([89–92]), although it is known in Russian literature as C-bifurcation.

However, to be more precise the C-bifurcation is typical for Filippov's systems [80], whereas grazing bifurcation is more practically oriented one and appears in systems with impacts. During investigations of maps a so-called border-collision bifurcation may appear, which is related to grazing bifurcation of a vector field ([41, 79, 80, 183, 185, 186]). Namely, it characterizes a collision of a mapping point with a discontinuity surface.

In Fig. 13.26 a grazing bifurcation is schematically shown for two different PSDS. Namely, a system with continuous vector state (Fig. 13.26a), and a system with a jump of a vector state (Fig. 13.26b) are displayed. The letter case is typical for impacting systems.

Although the classical grazing bifurcation assumes that a discontinuous surface in a contact place is smooth, but in practise very often it can be non-smooth. Imagine that a surface $\Sigma_{i,j}$ is composed of two smooth parts $\Sigma_{i,j}^{(1)}$ and $\Sigma_{i,j}^{(2)}$, which intersection creates a set C with dimension $(n-2)$, where n is dimension of phase space (see Fig. 13.27).

Two first bifurcations (Fig. 13.27a, b) belong to corner-collision bifurcation, whereas the third one Fig. 13.27c is more complicated.

Another important class of bifurcations exhibited by PSDS is associated with a sliding motion along $\Sigma_{i,j}$ (a trajectory remains on $\Sigma_{i,j}$ on a finite time interval). In the Filippov systems the vector field either forces the trajectories to move into $\Sigma_{i,j}$ from its both sides (attraction sliding mode) or to move away from it (repulsion sliding mode). More details are given in [46, 152].

In our example reported in Fig. 13.23c a real stick phase of the mass (which moves together with tape) can be referred as the attraction sliding mode.

When PSDS moves along a discontinuous surface a sliding type bifurcation can occur [46, 82]. In this case an orbit interacts with a part $\overline{\Sigma}$ of a discontinuity hyperplane Σ. Four different sliding bifurcations in Filippov's systems are reported in Fig. 13.28.

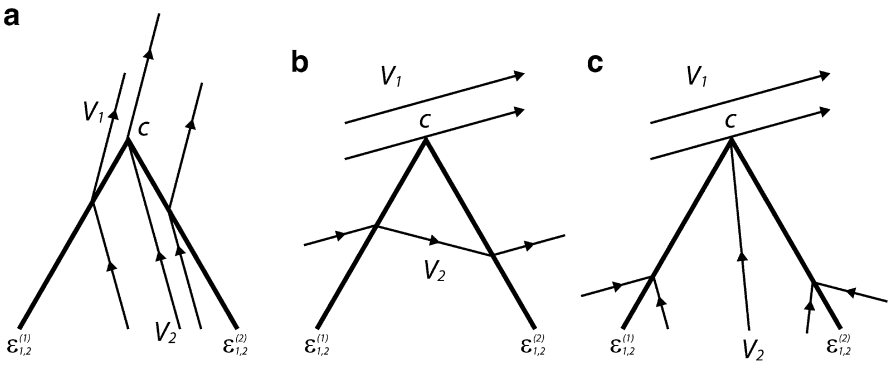

Fig. 13.27 Internal (**a**) and external (**b**) corner—collision bifurcation and bifurcation with sliding on $\Sigma^{(i)}_{1,2}$, $i = 1, 2$ (see [78])

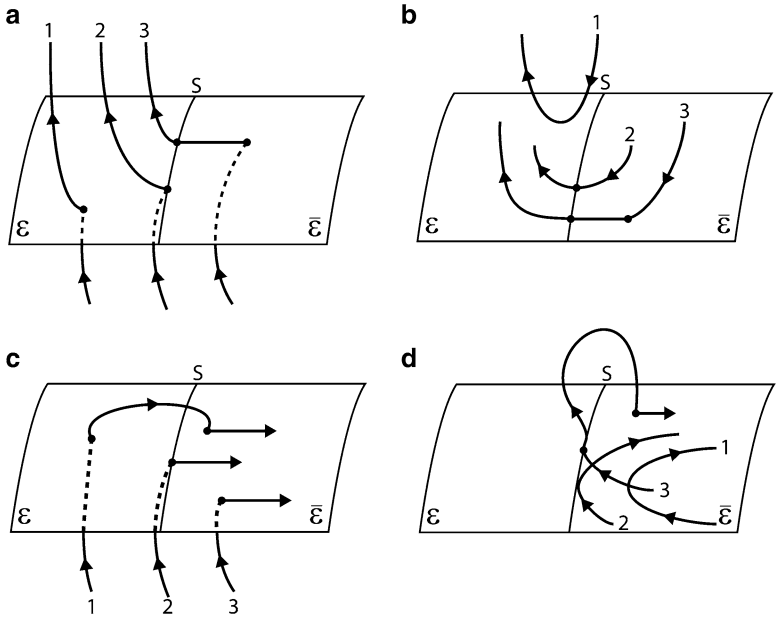

Fig. 13.28 Four different sliding bifurcations in a Filippov's system

Type I sliding bifurcation is shown in Fig. 13.28a. Increasing a bifurcation parameter the orbit first intersects transversally Σ, and then it moves to right successively touching the S-border between Σ and $\overline{\Sigma}$ (trajectory 2) and begins to slide. Any trajectory leaves $\overline{\Sigma}$ tangently.

In Fig. 13.28b the trajectory 1 approaches Σ and $\overline{\Sigma}$, it touches Σ and $\overline{\Sigma}$ simultaneously (orbit 2). Increasing further a bifurcation parameter a sliding part

on $\overline{\Sigma}$ occurs (see orbit 3). This bifurcation is said to be grazing-sliding and it generalizes a grazing bifurcation concept.

The third example (Fig. 13.28c) is referred as a sliding bifurcation of type II (sometimes it is also called switching-sliding).

First, the orbit 1 intersects transversally Σ. Two other orbits remain in $\overline{\Sigma}$. All of the orbits are associated with sliding out of the border S.

The last (Fig. 13.28d) type of sliding bifurcation is called multisliding. All orbits belong to $\overline{\Sigma}$. A change of a bifurcation parameter yields to partition of the orbit into two parts (one of it lies on $\overline{\Sigma}$, and the other one lies outside of $\overline{\Sigma}$). The described multisliding bifurcation is a member of a sliding adding scenario, which yields an occurrence of periodic orbits with increasing number of sliding intervals [81].

13.6.4 Bifurcations in Filippov's Systems

Filippov's systems belong to classes (i) and (ii) and they are characterized by systems with at least smooth vector state.

In [151, 152] bifurcations of periodic solutions in systems with discontinuous vector fields are analysed. Although it is assumed that the Poincaré section in a bifurcation point is continuous but not necessarily smooth. Assume that a being analysed periodic solution is in contact with a discontinuous surface Σ. If the perturbed orbit intersects Σ and moves into another part of the phase space, where it stays infinitely short time, and then it returns to the previous phase domain, then the associated Poincaré map is continuous. It can be proved that if the analysed periodic orbit in tangent to a smooth discontinuity surface, then the Poincaré map is smooth and its Jacobian is continuous. When the orbit goes through the point of discontinuity surface which is non-smooth, then the associated Jacobian is non-continuous. To omit the occurred problem a concept of a generalized Clarke's derivatives can be applied. It yields definitions of both generalized Jacobian and generalized fundamental matrix. It can be shown also that a generalized Jacobian can be obtained via linear approximation of a non-smooth vector field F in a thin phase space $\overline{\Sigma}$ with ϵ thickness including a surface of discontinuity Σ. In words, a non-continuous vector field F is substituted by continuous but non-smooth vector field $\tilde{F}$, when $\epsilon \to \infty$.

13.6.5 Bifurcations of Stationary Points

Consider first codimension 1 bifurcations of a fixed point $x^* = x^*_{\Sigma_{i,j}}$ of the vector field F lying on the non-smooth surface $\Sigma_{i,j}$, being a border between subspaces V_i and V_j, where F is smooth.

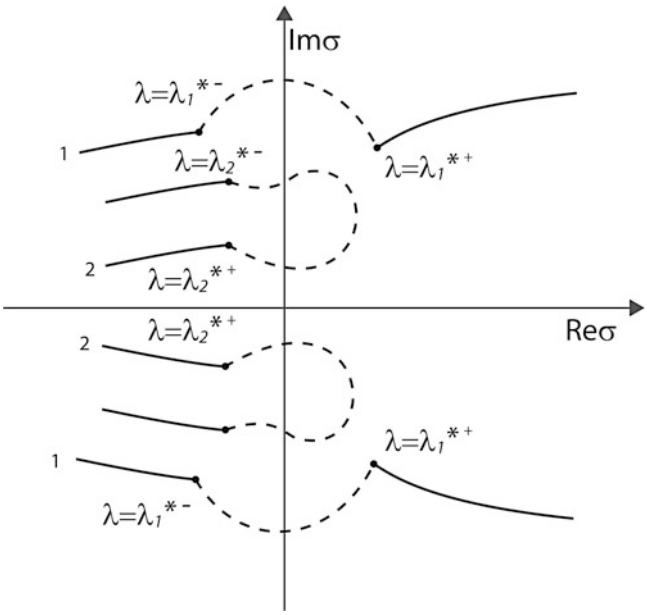

Fig. 13.29 Two different path of eigenvalues σ displaying discontinuous bifurcations

Since the point $x^*_{\Sigma_{i,j}}$ belongs simultaneously to V_i and V_j, it possesses two different values of a $DF_i(x^*_{\Sigma_{i,j}};\lambda_{\Sigma_{i,j}})$ and $DF_j(x^*_{\Sigma_{i,j}};\lambda_{\Sigma_{i,j}})$ on each of two sides of $\Sigma_{i,j}$. In what follows the following generalized Jacobian is defined in the point $x^*_{\Sigma_{i,j}}$:

$$\tilde{D}F(x^*_{\Sigma_{i,j}};\lambda_{\Sigma_{i,j}}) = (1-q)DF_i(x^*_{\Sigma_{i,j}};\lambda_{\Sigma_{i,j}}) + qDF_j(x^*_{\Sigma_{i,j}};\lambda_{\Sigma_{i,j}}), \qquad (13.207)$$

where $0 \leq q \leq 1$.

Formula (13.207) yields possible values of Jacobian in the point $x^*_{\Sigma_{i,j}}$ and it represents the smallest convex set possessing two values of Jacobian on two sides of $\Sigma_{i,j}$. Note that for $q = 0$ we have $\tilde{D}F(x^*_{\Sigma_{i,j}};\lambda_{\Sigma_{i,j}}) = DF_i(x^*_{\Sigma_{i,j}};\lambda_{\Sigma_{i,j}})$, whereas for $q = 1$ we get $\tilde{D}F(x^*_{\Sigma_{i,j}};\lambda_{\Sigma_{i,j}}) = DF_j(x^*_{\Sigma_{i,j}};\lambda_{\Sigma_{i,j}})$.

The mentioned set does not only define eigenvalues of Jacobians in a discontinuous point, but also defines a path of their jumps, when x^* goes through $\Sigma_{i,j}$. Now, if during such a jump the imaginary axis of the phase plane is crossed, then the associated bifurcation is called discontinuous one (see Fig. 13.29).

In the first case (curve 1) two complex conjugate eigenvalues cross once the imaginary axis, whereas in the second case (curve 2) the eigenvalues paths intersect the imaginary axis two times.

It is worth noticing that for each classical local bifurcation there exist also corresponding non-smooth bifurcations.

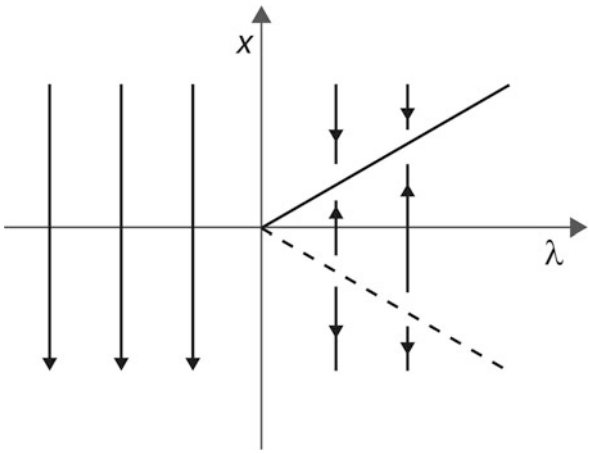

Fig. 13.30 Discontinuous saddle-node bifurcation

For instance, classical smooth saddle-node bifurcation can be displayed by the following equation

$$\dot{x} = F(x;\lambda) = \lambda - \mid x \mid . \tag{13.208}$$

The PSDS (13.208) does not contain fixed points for $\lambda < 0$, whereas for $\lambda > 0$ it has two fixed points $x^* = \pm\lambda$ (one of them is stable (solid curve), and one unstable (clashed curve)—see Fig. 13.30).

The generalized Jacobian computed in (0;0) is equal to $\tilde{D}F(0;0) = -2q + 1$ for $0 \leq q \leq 1$. The associated eigenvalue in the bifurcation point $\sigma = [-1, 1]$. For $q = 0 (q = 1)$ we have $\sigma = 1$ ($\sigma = -1$), whereas for $q = \frac{1}{2}$ we have $\sigma = 0$.

Although it is not difficult to construct the corresponding discontinuous partners to the classical smooth bifurcations, we consider only one more bifurcation of the following non-smooth system

$$\dot{x} = F(x;\lambda) = \pm x + \left| x + \frac{1}{2}\lambda \right| - \left| x - \frac{1}{2}\lambda \right| . \tag{13.209}$$

The system has three stationary points $x^* = 0$ (stable for $\lambda < 0$, and unstable for $\lambda > 0$), and $x^* = \pm\lambda$ with the marked stability in Fig. 13.31.

Since two non-smooth vector field surfaces appear in the point (0;0), two parameters q_i, i=1,2 are needed to define a generalized Jacobian $\tilde{D}F(0;0) = 2(q_2 - q_1) - 1$, where $0 \leq q_i \leq 1$. For $q_2 = q_1 + \frac{1}{2}$ the associated eigenvalue crosses the imaginary axis yielding the discontinuous pitchfork bifurcation.

One may also construct a discontinuous Hopf bifurcation, which is governed by two following non-smooth equations

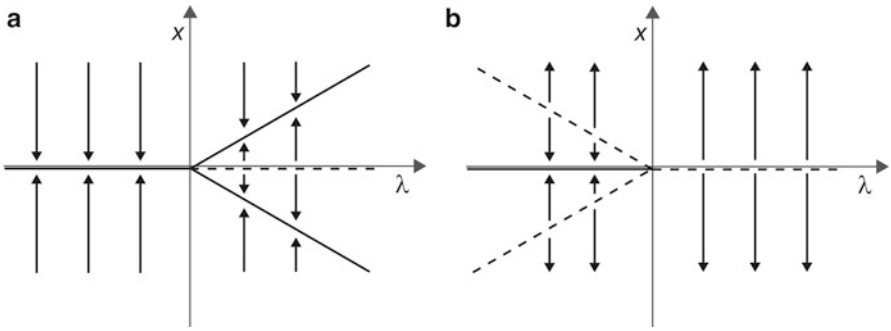

Fig. 13.31 Discontinuous pitchfork bifurcation (supercritical (**a**) and subcritical (**b**))

$$\dot{x}_1 = -x_1 - \omega x_2 + \frac{x_1}{\sqrt{x_1^2 + x_2^2}} \left(\left| \sqrt{x_1^2 + x_2^2} + \frac{1}{2}\lambda \right| - \left| \sqrt{x_1^2 + x_2^2} - \frac{1}{2}\lambda \right| \right),$$
$$\dot{x}_2 = \omega x_1 - x_2 + \frac{x_2}{\sqrt{x_1^2 + x_2^2}} \left(\left| \sqrt{x_1^2 + x_2^2} + \frac{1}{2}\lambda \right| - \left| \sqrt{x_1^2 + x_2^2} - \frac{1}{2}\lambda \right| \right). \tag{13.210}$$

Introducing the transformation

$$x_1 = r\cos\Theta, \qquad x_2 = r\sin\Theta \tag{13.211}$$

one gets

$$\begin{aligned} \dot{r} &= -r + \mid r + \tfrac{1}{2}\lambda \mid - \mid r - \tfrac{1}{2}\lambda \mid, \\ \dot{\Theta} &= \omega. \end{aligned} \tag{13.212}$$

For $\lambda < 0$ the stationary point $[x_1, x_2]^T = [0; 0]^T$ is stable, whereas for $\lambda > 0$ it becomes unstable, and a new stable periodic solution with the amplitude $r = \sqrt{x_1^2 + x_2^2}$ appears (a supercritical bifurcation).

13.6.6 Bifurcations of Periodic Orbits

A similar idea of generalized derivative can be used to trace periodic orbits yielded by a non-smooth vector field. A so-called generalized fundamental matrix is defined via relation

$$\tilde{\phi} = (1 - q)\phi^- + q\phi^+, \tag{13.213}$$

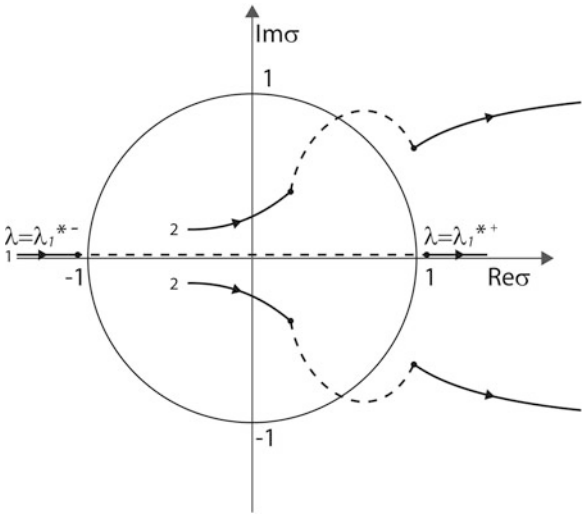

Fig. 13.32 Two paths of eigenvalues during fold-flip (*2*) and Neimark–Sacker (*1*) discontinuous bifurcations

where $0 \leq q \leq 1$. For $\lambda = \lambda^*$ we have two values $\phi = \phi^-$ or $\phi = \phi^+$ ($\phi^- = \lim\limits_{\substack{\lambda \to \lambda^* \\ \lambda < \lambda^*}} \phi$; $\phi^+ = \lim\limits_{\substack{\lambda \to \lambda^* \\ \lambda > \lambda^*}} \phi$). Two typical discontinuous bifurcations, i.e. Neimark–Sacker and fold-flip are shown in Fig. 13.32.

The unit circle of complex eigenvalues plane is crossed via a jump by a pair of complex conjugated eigenvalues and it is referred as the discontinuous Neimark–Sacker bifurcation. A real eigenvalue can jump from inside of the unit circle through either -1 (discontinuous period doubling or flip bifurcation) or through $+1$ (fold bifurcation). However, a real eigenvalue $\sigma < -1$ can also jump over the circle getting new value $\sigma > 1$. This discontinuous bifurcation is called fold-flip (path 1 in Fig. 13.32).

The described simple smooth and they corresponding non-smooth bifurcations have relatively simple geometrical interpretation (see Fig. 13.33).

One-dimensional Poincaré map in the vicinity of smooth saddle-node bifurcation (Fig. 13.33a) does not intersect the line $x_{i+1} = x_i$ for $\lambda < \lambda^*$, is tangent to this line for $\lambda = \lambda^*$, and possesses two intersection points for $\lambda > \lambda^*$ (the last case corresponds to two periodic orbits of an associated dynamical system). The Poincaré map of non-smooth saddle-node bifurcation touches $x_{i+1} = x_i$ in non-smooth point (cusp), and hence it has different left-hand side and right-hand side derivatives.

In Fig. 13.33b for smooth period doubling bifurcation one-dimensional Poincaré map intersects $x_{i+1} = x_i$ in the point, where the associated derivative is equal to -1. On the other hand, in the case of non-smooth period doubling bifurcation (dashed lines) the associated Poincaré map intersects $x_{i+1} = x_i$ in the cusp and it has two different values of a derivative.

To sum up, the situation of classification of possible non-smooth bifurcations is far to be completed. As it has been already mentioned, such bifurcation may have their analogues in classical smooth bifurcations or they can be combinations

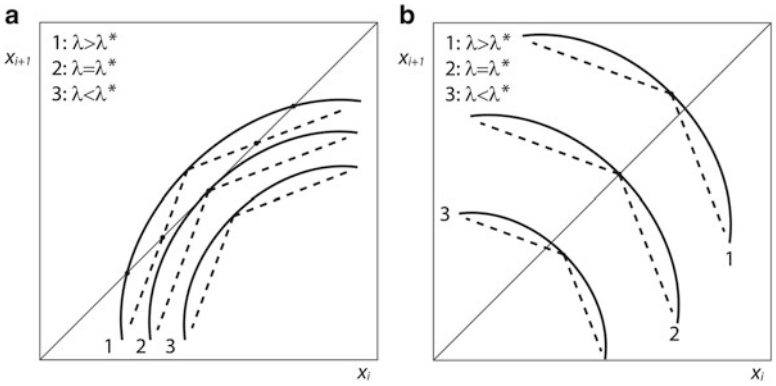

Fig. 13.33 Poincaré maps displaying saddle-node (**a**) and period doubling (**b**) smooth (*solid curve*) and non-smooth (*dashed lines*) bifurcations

of a sequence of such smooth bifurcations. However, there are also non-smooth bifurcations which have not their analogy in smooth systems.

The earlier briefly described C-bifurcations or border collision bifurcation are also locally analysed using piecewise smooth local modes in [78–80, 82, 92]. The popular grazing bifurcation is classified through estimation of real eigenvalues of a map, which are less than -1 and larger than $+1$ on both sides of a discontinuity. However, the Neimark–Sacker bifurcation is not discussed.

Almost nothing is done in the field of global non-smooth bifurcations and local non-smooth bifurcations occurred in high dimensional systems.